

We appreciate both reviewers for their helpful comments and suggestions concerning our research. We revised the manuscript accordingly. We present our response and changes below. Reviewers' comments and suggestions are shown in *italic*. Authors' responses are in **bold**.

Response to Referee #1:

Summary:

Zhang et al. use the REAM chemistry transport model simulation to investigate transport of aromatics to the Tibetan plateau. Their work shows that the INTEX-B 2006 emissions of aromatics do not produce sufficient glyoxal concentrations compared to the SCIAMACHY retrieval. The authors apply a top-down estimate to update the emissions of aromatics, which are glyoxal precursors. The REAM model results of aromatics were compared with observations taken at several ground locations over a 3-week period. Samples in central Tibet had the highest aromatic concentrations and were attributed to meteorological conditions that increased southwesterly surface winds bringing high concentrations of aromatics from the Indo-Gangetic Plain to Tibet. The complex topography of this region makes for an especially challenging effort to represent transport into Tibet.

The investigation is important in terms of understanding transport of pollutants, especially black carbon, from population and industrial regions to the Himalayan glaciers. The results from this paper suggest the critical need to represent the airflow in complex terrain to predict black carbon transport accurately. While these conclusions are not unfamiliar, it is important to continue to highlight the role of meteorology on transport of pollutants. The presentation of the investigation is fair. One can understand the points being made, but it is not written as a compelling story. Several of the points below suggest ways to improve the paper.

A main focus of this research is to show the enhanced trans-Himalaya transport towards Tibet in the presence of the cut-off low system. We apply the top-down emission estimate technique and find that the model underestimates of reactive aromatics during Period 2 result from the underestimation of the emission inventory. The WRF simulated and the observed meteorology fields show that the rise of reactive aromatics concentrations during October 21-24 is related to the cut-off low system. We further analyze the geopotential heights and compare WRF simulated and observed surface winds during Period 1. The results imply a missing cut-off low system during Period 1, which is not captured by the 36km resolution WRF model. It will be more challenging for climate models with coarser resolutions to capture the cut-off low systems. Thus, we suggest climate model results of trans-Himalaya transport of pollutants (including BC) must be evaluated with our findings in mind. Last, we point out that the model underestimation during Period 3 is due to the effects of complex terrains.

Major Comments

1. Aromatics are good markers of transport that occurs over 1 day period because of their chemical lifetime. However, aromatics are not subject to wet deposition because of their low solubilities (Sander, 2015), while black carbon can be removed by storms. Therefore, it makes sense to use aromatics to analyze transport (isolating the one process), but they are not good proxies for black carbon. The authors should explain this caveat in the paper.

Although air mass transport towards north of the Himalayas is enhanced during the presence of the cut-off low system, different species share various physical and chemical processes and are affected by the cut-off low system to different extents. Compared to aromatics, black carbon (BC) transport is also subject to wet scavenging, the efficiency of which depends on the hygroscopicity of BC. For freshly emitted BC from the industrialized Indo-Gangetic Plain (IGP), the scavenging effect requires in situ

observations. Nonetheless, trans-Himalaya transport during October 21-24 is clearly much faster than that during October 19-20. If this process is not simulated correctly in the model, BC transport from India to Tibet will likely be underestimated. Further, Fig. S6 in the Supplement shows that the precipitation distribution for October 19-20 and October 21-24. The cut-off low system and associated precipitation are to the northwest of Tibet. Precipitation south of Tibet is weak and thus the subsequent removal of BC during trans-Himalaya transport is limited.

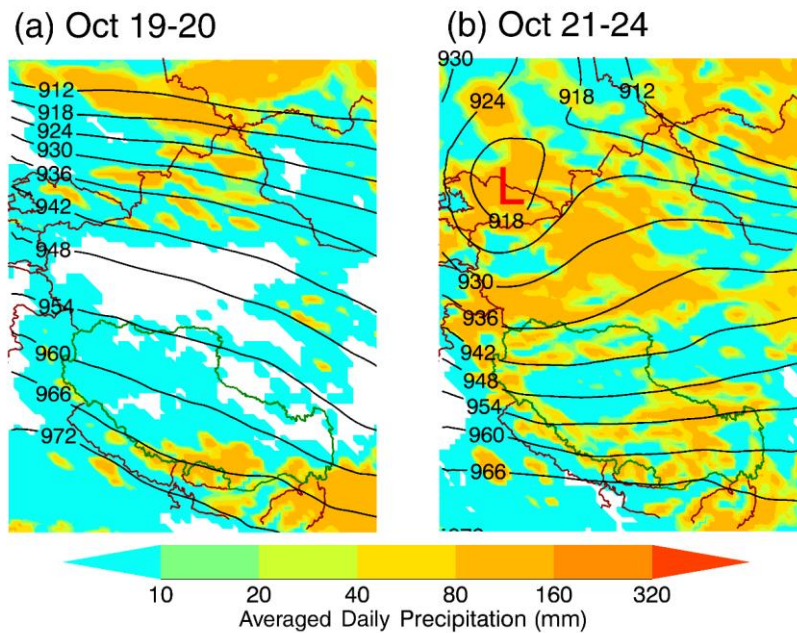


Figure S6: WRF simulated averaged daily precipitation for October 19-20 (a) and October 21-24 (b), respectively.

In addition, we conducted a sensitivity simulation in order to address the sensitivity of our modeling results to the emission distribution difference between aromatics and BC. We redistributed the total aromatics emissions over China and other South Asia countries on the basis of the BC emission distribution. The resulting aromatics emissions distribution resembles that of BC. We compare the source contribution results using original and the redistributed aromatics emissions (Fig. S7). Transport of BC from South Asia clearly dominates over Tibet during the cut-off low event (October 21-24).

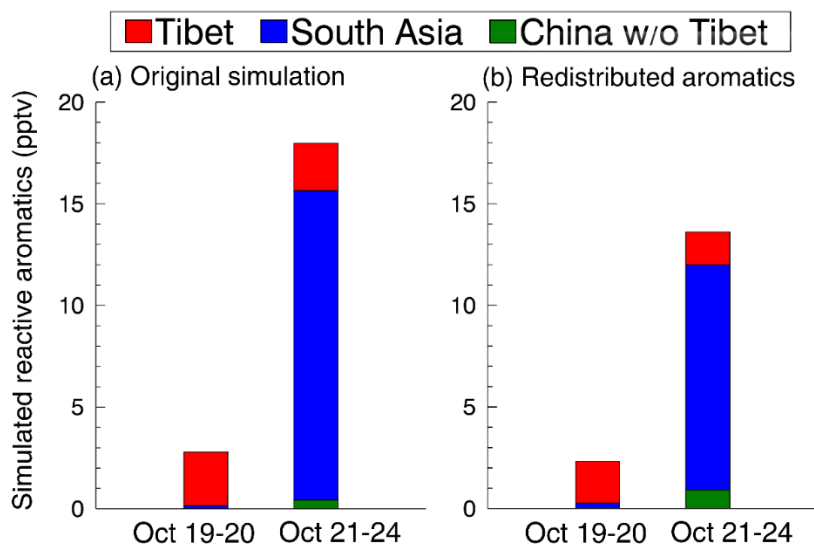


Figure S7: Averages of simulated reactive aromatics emitted from Tibet (red), India and nearby countries (“South Asia”, blue) and China excluding Tibet (“China w/o Tibet”, green) corresponding to in situ observations during October 19-20 and October 21-24. REAM simulations are conducted with original emissions (a) and the aromatics emissions redistributed following the BC emission distribution (b), respectively.

Thus, we conclude that the BC transport is enhanced by the cut-off low. We now clarify these issues in Section 3.3 as follows:

“Compared to aromatics, BC is also subject to wet scavenging, which greatly reduces its transport efficiency by convection. During our analysis period, the cut-off low system and the associated precipitation are to the northwest of Tibet (Fig. S6 in the Supplement). Precipitation south of Tibet is weak and thus the subsequent removal of BC during trans-Himalaya transport is limited.

To examine the sensitivity of trans-Himalaya transport to the distribution of emission sources, we redistribute INTEX-B the total aromatics emissions over China and other South Asia countries on the basis of the MIX BC emission distributions. We conduct a sensitivity simulation using the redistributed emissions and compared the results to the original simulation. The trans-Himalaya transport from South Asia clearly dominates and it is strongly affected by the presence of a cut-off low system during our analysis period (Fig. S7 in the Supplement). Our analysis implies that BC transported in the presence of an upper tropospheric cut-off low is potentially a major contributor to BC deposition to Tibetan glaciers.”

2. There is a lack of recognition of previous studies, especially of regional chemistry transport modeling in South Asia and western China. Some previous papers to consider are listed in the references.

We did another search of related literature and discussed the relevant studies:

“The deposition of BC on the vast glaciers of the Tibetan Plateau will decrease the surface albedo, accompanied by increased sunlight absorption and subsequent enhanced melting (Hansen and Nazarenko, 2004; Ramanathan and Carmichael, 2008; Ming et al., 2009; Yasunari et al., 2010). Increasing BC concentrations were previously found in ice core and lake sediment records (Xu et al., 2009; Cong et al., 2013). The dwindling of glaciers over Tibet is a major concern for fresh water supply to a large portion of the Asian population through the Indus River, Ganges River, Yarlung Tsangpo River, Yangtze River and Yellow River (Singh and Bengtsson, 2004; Barnett et al., 2005; Lutz et al., 2014). Though melting glaciers favor river runoff temporarily, mass loss of glaciers endangers water supply during the dry season in the future (Yao et al., 2004; Kehrwald et al., 2008).

Increasing BC concentrations were already found in ice core and lake sediment records (Xu et al., 2009; Cong et al., 2013). Besides narrowing the uncertainties of BC emissions, aging and deposition, better understanding the transport pathways are equally important in this region. Surrounded by the largest ~~black carbon~~ BC sources of East Asia and South Asia (Bond et al., 2007; Ohara et al., 2007), Tibet is primarily affected by pollutant transport from these two regions (Kopacz et al., 2011; Lu et al., 2012; Zhao et al., 2013; Wang et al., 2015; Zhang et al., 2015); Li et al., 2016; Wang et al., 2016; Kang et al., 2016). Kopacz et al. (2011) attempted to identify the sources of BC over glaciers in the Himalayas and the Tibetan Plateau (HTP) using the adjoint model of GEOS-Chem. Lu et al. (2012) developed a novel back-trajectory model with BC emissions, hydrophilic-to-hydrophobic aging, and deposition and found that South Asia and East Asia account for 67% and 17% of BC over the HTP. Using source tagging, biofuel and biomass burning emissions from South Asia are found to be the largest sources of BC in HTP followed by fossil fuel combustion emissions (Zhang et al., 2015). Hindman and Upadhyay (2002) ~~proposed~~suggested that the vertical lifting due to convection and subsequent horizontal mountain-valley wind lead to the transport of ~~condensation nuclei~~aerosols from Nepal to Tibet. ~~Cong et al.~~Dumka et al. (2010) also stressed the importance role of mountain-valley wind in BC concentration in Central Himalayas. Cong et al. (2015) suggested that both the large-scale westerlies from EastSouth Asia and the local mountain-valley wind from South Asia are major transport pathways. The synoptic scale trough and ridge can potentially lead to the trespassing of atmospheric brown clouds from South Asia to the Tibetan Plateau (Lüthi et al., 2015). Ji et al. (2015) indicated that the southwesterlies during monsoon season favor aerosols transport across the Himalayas from South Asia. Aerosols observations in previous studies are mostly limited to the southern and northern slopes of the Himalayas (Hindman and Upadhyay, 2002; Dumka et al., 2010; Cong et al., 2015) with very few in situ sites (e.g. Namco, Linzhi) inside Tibet (Kopacz et al., 2011; Ji et al., 2015; Lüthi et al., 2015; Zhang et al., 2015). Considering the complex topography (Lawrence and Lelieveld, 2010; Ménégos et al., 2013; He et al., 2014; Kumar et al., 2015) and scarce observations (Maussion et al., 2011), it is crucial to evaluate model simulated transport performance over the Tibetan Plateau using available observations with a good spatial coverage. Observation-constrained modeling, ~~however,~~ is needed to better understand potential model biases: due to the uncertainties of model simulated transport from South Asia to Tibet.”

3. When figures are discussed in enough detail, it is better to place them in the main part of the paper. In my opinion, the supplement should not contain information that is needed to support the conclusions of the paper. For example, Figure S2 should be part of the main paper because it supports the conclusion that the INTEX-A aromatics emission estimates are much lower than values determined from a top-down estimate. Please write the paper so that the reader can easily understand the main points of the study.

Thank you for the suggestion. We now combined Fig. S2 and Fig. 2. Please note that we did not use INTEX-A emission estimates in this work. Only INTEX-B data are used. Per reviewer's suggestion (see the response below), we updated emissions using the MIX inventory (please see updates in section 2.3).

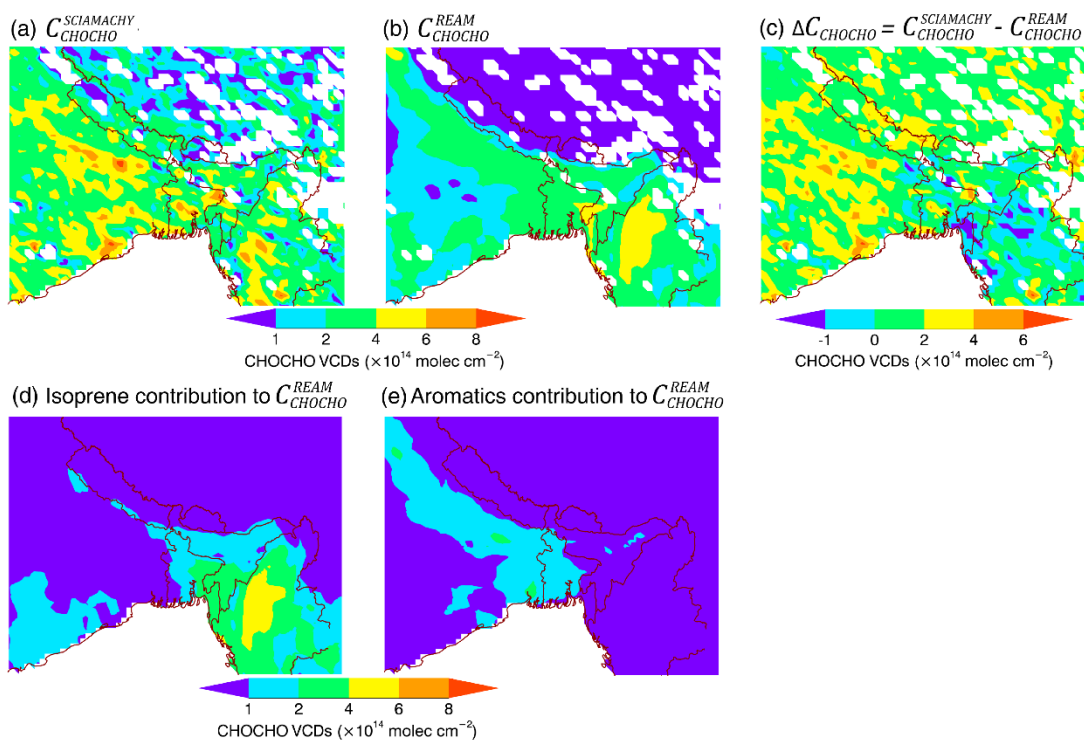


Figure 2: SCIAMACHY observed CHOCHO VCDs (a) and, REAM simulated (b) CHOCHO VCDs, the low bias of simulated CHOCHO VCDs (c), simulated isoprene (d) and aromatics (e) contributions to CHOCHO VCDs using the a priori emissions for October 2010. White areas in the observations denote missing satellite data or ocean. For each valid SCIAMACHY data point, a corresponding model value is sampled in (b) and (c).

Minor Comments:

1. Page 4, Line 1: How does one choose α for use in the uncertainty equation? Is this even necessary information for the reader?

The range of α shows the relative uncertainty of SCIAMACHY glyoxal (CHOCHO) VCDs. This will help readers understand that the retrieval uncertainty cannot explain the discrepancy between observed and simulated CHOCHO VCDs. This stresses the needs for the top-down emission estimate.

We add the following sentence to Section 2.4.

“First, we calculate the difference between observed ($C_{\text{CHOCHO}}^{\text{SCIAMACHY}}$, Fig. 2a) and modeled ($C_{\text{CHOCHO}}^{\text{REAM}}$, Fig. 2b) CHOCHO VCDs with original emissions ($\Delta C_{\text{CHOCHO}} = C_{\text{CHOCHO}}^{\text{SCIAMACHY}} - C_{\text{CHOCHO}}^{\text{REAM}}$, Fig. [S2a—in Supplement-2c](#)). This discrepancy greatly exceeds the uncertainties of SCIAMACHY retrieval.”

2. I suggest rearranging the model description paragraphs. How would you describe the model to someone who has never worked with regional transport models? I suggest beginning with the CFSR dataset because it is used to provide initial and boundary conditions for the WRF model. Then the WRF model should be described, citing what version, resolution, and parameterizations are used. Next, it should be stated how REAM takes information from the WRF simulation. Does it take WRF output every hour, every 3 hours, etc.? Finally, the REAM model should be described. Do not rely on the reader to go to the cited references to get needed information, but instead to go to the cited references to get more details.

Thank you for the suggestion. We now add more details of the model.

“REAM has a horizontal resolution of 36 km with 30 vertical levels in the troposphere and 5 vertical levels in the stratosphere covering adjacent regions of China (Fig. 4a1b). The model top is at 10 hpa. Meteorological fields in REAM are obtained from the Weather Research and Forecasting model (WRF) assimilations constrained by National Centers for Environmental Prediction Climate Forecast System Reanalysis (NCEP CFSR, Saha et al., 2010) 6-hourly products, which have a horizontal resolution of T382 (~38 km). We run the WRF model with the same resolution as in REAM with a domain ~~is~~ larger than that of REAM by 10 grid cells on each side. Meteorological inputs related to convective transport are updated every 5 minutes while the others are updated every 30 minutes. The recent update of REAM expands the GEOS-Chem standard chemical mechanism (V9-02) to include a detailed description of ~~aromatic~~aromatics chemistry (Bey et al., 2001; Liu et al., 2010, 2012b). Aromatics are lumped into three species based on reactivity, i.e. ARO1 (toluene, ethyl-benzene), ARO2 (m/p/o-xylene), and benzene. The atmospheric lifetimes of the three aromatics tracers against OH are 18 hours, 4.2 hours and 3.9 days during the study period (October 13-25, 2010), respectively. Due to the long atmospheric lifetime of benzene, it is more difficult to track and identify its sources; thus we do not explicitly discuss benzene in this study. We focus our analysis on reactive aromatics (toluene, ethyl-benzene, and m/p/o-xylene).

~~Meteorological fields in REAM are obtained from the Weather Research and Forecasting model (WRF) assimilation constrained by National Centers for Environmental Prediction Climate Forecast System Reanalysis (NCEP CFSR, Saha et al., 2010). CFSR has a horizontal resolution of T382 (~38 km). Initial and boundary conditions for chemical tracers are taken from GEOS-Chem (V9-02) 2° × 2.5° simulation- (Bey et al., 2001).”~~

3. *It is important to include what the model top is because of the high surface elevation of Tibet that is prone to have stratospheric intrusions (perhaps falsely if the model top is too low).*

The model top is 10 hpa, which is above the tropopause. REAM has 30 layers in the troposphere and 5 layers in the stratosphere. So it should be able to resolve stratospheric intrusions. We added this information to Section 2.3.

“REAM has a horizontal resolution of 36 km with 30 vertical levels in the troposphere and 5 vertical levels in the stratosphere covering adjacent regions of China (Fig. 4a1b). The model top is at 10 hpa.”

4. *Has the REAM model been evaluated for the region simulated? In this paper we see comparisons with SCIAMACHY and ground-based observations. How does the model perform in terms of meteorology and chemical constituents, such as CO, O3, NOx, and particulate matter?*

Unfortunately, we do not have many in situ observations in the region (in particular Tibet) to evaluate the model. In the introduction section, we discussed previous studies and noted the lack of in situ observations over Tibet (very few surface sites). The dataset reported in this study provides valuable information over the Tibetan Plateau. In an effort to respond to reviewer’s comment, we make a comparison with available satellite products. It appears that REAM simulated NO₂ and CO compared reasonably well with KNMI DOMINOv2 tropospheric NO₂ VCDs (<http://www.temis.nl/airpollution/no2col/>) and MOPITT daytime total CO VCDs (<http://www.acom.ucar.edu/mopitt/MOPITT/>) for Tibet, India and nearby regions (Fig. S2) during the period of the study. For the general evaluation of the model, we refer to other publications using REAM cited in Section 2.3.

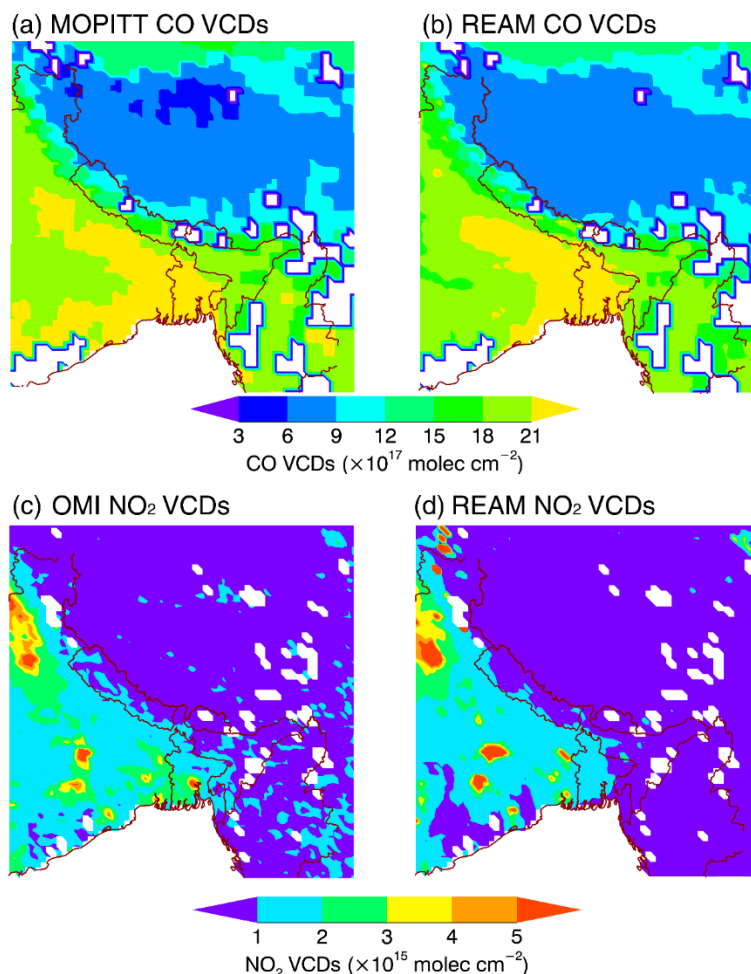


Figure S2: MOPITT retrieved (a) and REAM simulated (b) monthly averaged total CO VCDs during October 2010. OMI retrieved (c) and REAM simulated (d) monthly averaged tropospheric NO₂ VCDs during October 2010. White areas denote missing data. MOPITT data are from <http://www.acom.ucar.edu/mopitt/MOPITT/>. OMI data are from <http://www.temis.nl/airpollution/no2col/>. Averaging kernels are applied to the model results.

We now discuss REAM performance in Section 2.3:

“Compared with satellite observed CO and NO₂ VCDs, REAM performs reasonably well in the study region during October 2010 (Fig. S2 in the Supplement). For general model evaluations of REAM, we refer the readers to the papers cited early in this section.

We updated the INTEX-~~b~~B emission inventory in South Asian countries through inverse modeling constrained by SCIAMACHY CHOCHO VCDs (Section 2.4 next section).”

5. The model domain is shown in Figure 1, allowing the reader to recognize that the region of interest is mostly away from the model boundaries. Is the Tibet region affected by the composition outside the model boundaries (especially the western boundary), or outside the subdomain shown in Figure 2?

Since the regions outside the model boundary are either remote or too far away from the studied regions, the contributions from these regions to both glyoxal and aromatics are negligible. Also, we use the concentrations from a global chemistry transport model (GEOS-Chem) as our boundary conditions.

6. When comparing the REAM model results with the SCIAMACHY satellite retrieval of glyoxal, is the model sampled the same way as SCIAMACHY sees the atmosphere?

For example, I assume that the missing data in Figure 2a from the satellite data is due to clouds. Are cloudy grid points removed from the model analysis (it doesn't appear so since there are no "missing data" from the model results).

We resampled REAM in the results in Fig. 2 (shown in major comment #2). We added in the caption of Fig. 2 "For each valid SCIAMACHY data point, a corresponding model value is sampled in (b) and (c)." Interferences of clouds and water vapor have been removed in the SCIAMACHY retrieval. The missing data in satellite retrieval results from quality control in retrieval algorithm, which can result from excessive cloud coverage, large uncertainty and measurement failure. Glyoxal VCDs in Tibet are very low and the relative error is large. Consequently, these values are removed. Considering the retrieval uncertainties over the Tibetan Plateau, we only perform top-down emission inversion in regions south of the Himalayas.

7. Page 5, Line 21. *It would be helpful to see a MEGAN emissions map of isoprene for the region.*

We revise this sentence "The high isoprene contribution to glyoxal VCDs is to the southeast of the Indo-Gangetic Plain, where CHOCHO VCDs are high in both the observations and model simulations." Fig. 2d shows the contribution from isoprene to glyoxal VCDs.

8. Page 5, Lines 16-24. *It may be helpful to include the glyoxal chemistry in the supplement.*

We stated "CHOCHO is produced primarily from the photochemical oxidation of biogenic compounds (e.g., isoprene and terpenes) and hydrocarbon released by anthropogenic activities (e.g., acetylene, ethylene, and aromatics) (Fu et al., 2008)." The relevant chemistry is already discussed by Fu et al. (2008).

9. Section 2.4. *Why is the INTEX-B emissions inventory, which is appropriate for year 2006, being used for the model simulation for year 2010? MACCity emissions (appropriate for 2010) or EDGAR-HTAP emissions may have been better suited for these simulations. Could the authors discuss the differences between the emissions inventory that they used and these more recent emissions inventories?*

Thank you for the suggestion. We currently use MIX emissions inventory (Li et al., 2015) with INTEX-B aromatics emissions for countries other than China. HTAP-EDGAR now incorporates MIX for Asian emissions. MIX is mosaic emission inventory with MEIC for China and several other emission inventories for other countries. In addition to the MIX inventory, we also conduct sensitivity simulations using the Intercontinental Chemical Transport Experiment-Phase B (INTEX-B) emissions inventory (Zhang et al., 2009; Li et al., 2014), which was developed for the year 2006. We find that compared to the in situ observations of aromatics, the simulation results using the INTEX-B emissions are better. The main reason for the simulation improvements is due to the emissions of aromatics in South Asia. Given the large uncertainties in the emissions of aromatics (e.g., Liu et al., 2012b), this result is not surprising. Since MEIC and INTEX-B inventories are developed by the same group, we replace MIX aromatics emissions outside China with INTEX-B data such that aromatics emissions in the model are consistent. The improvements of model simulations compared to in situ observations are shown in Fig. S1. Since satellite observations are used to improve aromatics emissions (next section), using either MIX or INTEX-B emissions in this work gives the same conclusions.

MACCcity emissions inventory is a linear combination of Atmospheric Chemistry and Climate Model Intercomparison Project (ACCMIP) and Representative Concentration Pathway (RCP) 8.5. MACCcity is essentially RCP 8.5 for year 2010 and is not suitable for this research.

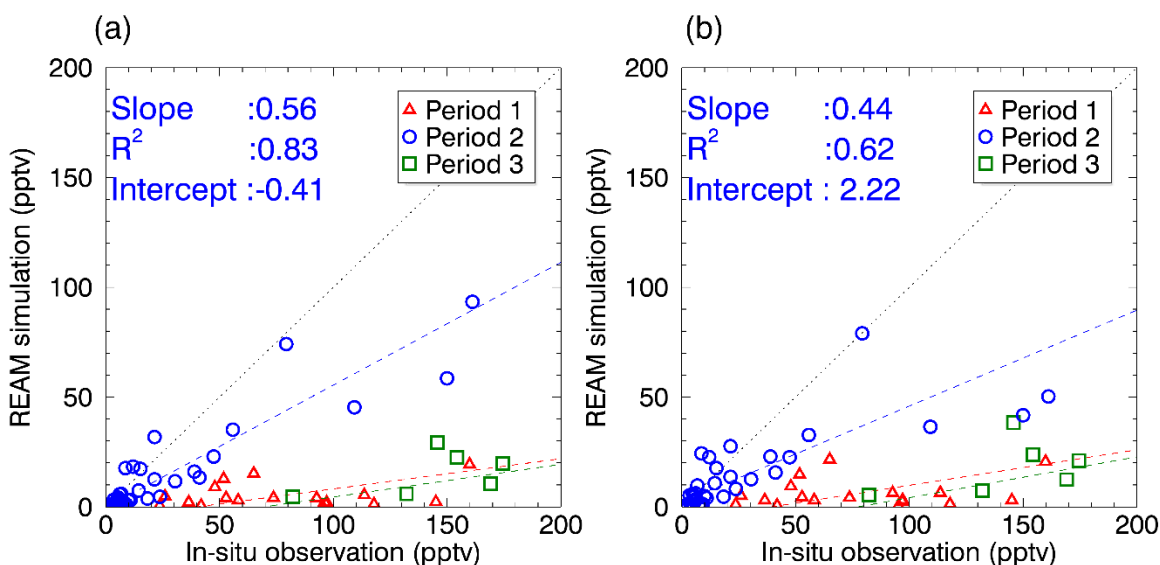


Figure S1: Comparisons between REAM simulated and in-situ observed reactive aromatics concentrations with (a) and without (b) INTEX-B aromatics emissions for countries excluding China.

We now discuss the use of emission inventories in Section 2.3 as follows.

“Initial and boundary conditions for chemical tracers are taken from GEOS-Chem (V9-02) $2^\circ \times 2.5^\circ$ simulation- (Bey et al., 2001). Anthropogenic emissions in China and other Asian countries are from the are from the MIX inventory for October 2010 (Li et al., 2015). MIX is a mosaic Asian anthropogenic emission inventory with the Multi-resolution Emission Inventory for China (MEIC-v1.0) for 2010 and updated-) for China and several other emission inventories for other Asian countries. In addition to the MIX inventory, we also conduct sensitivity simulations using the Intercontinental Chemical Transport Experiment-Phase B (INTEX-B) emission for 2006 (emissions inventory (Zhang et al., 2009; Li et al., 2014), respectively- which was developed for the year 2006. We find that compared to the in situ observations of aromatics, the simulation results using the INTEX-B emissions are better. The main reason for the simulation improvements is due to the emissions of aromatics in South Asia. Given the large uncertainties in the emissions of aromatics (e.g., Liu et al., 2012b), this result is not surprising. Since MEIC and INTEX-B inventories are developed by the same group, we replace MIX aromatics emissions outside China with INTEX-B data such that aromatics emissions in the model are consistent. The improvements of model simulations compared to in situ observations are shown in Fig. S1 in the Supplement. Since satellite observations are used to improve aromatics emissions (next section), using either MIX or INTEX-B emissions in this work gives the same conclusions.”

10. Section 3.1. It would be interesting to learn in more detail what the surface elevation is at the observation points and at the matching REAM model grid cells. Could there be discrepancies between model and observations because the model does not adequately represent the surface elevation?

The surface elevations between WRF results and observation during Periods 1 and 2 are similar. This is not surprising considering the generally smooth topography in these regions. We expect the winds to vary little within a WRF grid in such regions. As Fig. 7 shows, WRF simulated winds match in-situ

observations during Period 2. We suggest that the underestimation of WRF winds during Period 1 results from a missing cut-off low system. We also discuss the potential relationship between observed reactive aromatics and standard deviations of surface elevations during Period 3 in Section 3.4, the latter region has more variable topography than Periods 1 and 2. We suggest that the underestimation of the model results from model incapability to resolve complex terrains.

11. Page 7, Line 6. How are the source attributions computed?

For the sensitivity simulations, we only turn on aromatics emissions in one of the three regions, i.e. Tibet, other provinces of China and India and nearby regions. All the sensitivity simulations utilize OH concentrations specified to the archived values of the full model simulation using top-down emissions. The results from these simulations are used to calculate the source attributions.

We now clarify this in Section 2.3.

“We further carried out three model sensitivity tests to calculate the contributions to surface aromatics from emissions over Tibet, other provinces of China, and South Asia (India and nearby regions). Each simulation is run with only the aromatics emissions from the corresponding region. The OH concentrations in each simulation are specified to the archived values of the full model simulation. The results for two sub-periods of Period 2 are examined in Section 3.3.”

12. Page 7, Lines 15-17. Could the “cutoff low system” be described in more detail? Would “closed low” be a more appropriate term? (see the NWS definition at <http://forecast.weather.gov/glossary.php?word=cutoff%20low>) How long did the cutoff low remain in the region? Was there precipitation associated with the cutoff low?

Thanks for the reference. This low system became fully detached from the westerlies after generation. The cut-off system stayed for about 3 days and dissipated. The cut-off system and associated precipitation are to the northwest of Tibet (Fig. S6b in the Supplement). We add clarification in Section 3.3.

“During October 21-24, the presence of a southeastward-moving upper tropospheric cut-off low system induces increasingly stronger surface wind from India to Tibet (Fig. 5b, Hoskins et al., 1985). The cut-off low system is a closed low-pressure system detached from the westerlies. It began to form on October 21 and started to dissipate on October 24.”

13. Page 7-8. It would be helpful to see Figure S5 showing both Period 1 and Period 2. From what is presented, it is unclear whether WRF simulates the cutoff low pressure system (unless these are WRF results, which is not clear from the figure caption).

Fig. 5 shows the results for Period 2. In Fig. S8 (previously Fig. S5), both CFSR and CFSR-constrained WRF show a trough rather than a cut-off low system (Fig. 5) in Central Asia during Period 1.

14. Page 8, End of section 3. There should be a section added, discussing the results found in this study with previous papers (such as those listed in the references). For example, the Kumar et al. (2015) study also mentions the challenges of modeling pollutant transport in the Himalayas. Ji et al. (2015) also discuss aerosol transport from the IGP to Tibet.

We now discuss the related previous researches in Sections 3.3 and 3.4, respectively.

Section 3.3:

“Accompanying this transport, large amounts of pollutants such as reactive aromatics analyzed here are transported to the Tibetan Plateau leading to much higher surface concentrations.

The cut-off low system provides a more rapid and efficient pollutants transport pathway compared with transport pathways previously proposed by other studies, such as westerlies (Cong et al., 2015; Ji et al., 2015) and mountain-valley winds (Hindman and Upadhyay 2002; Dumka et al., 2010).”

Section 3.4:

“Model resolution as high as 1 km appears to be necessary to capture the observed feature but the computational resource requirement will be exceptionally large for a global model such as that used for CFSR. Other issues related to complex terrains in this region were also discussed by previous studies (Maussion et al., 2011; Ménégoz et al., 2013; He et al., 2014; Kumar et al., 2015).”

15. Figure 5. What is the source of the information plotted in Figure 5? Is it from the model (WRF + REAM) simulation? Please clarify. Why are the surface winds and simulated reactive aromatics shown only for Tibet?

Yes, the winds and geopotential heights come from WRF simulation while simulated reactive aromatics are REAM simulation results. We clarified this in the revised paper.

Fig. AR1 (below) shows surface winds and simulated reactive aromatics for the whole region. The surface winds can be misleading due to the high altitude of the Tibetan Plateau compared with surrounding regions.

To help readers focus on the study region and avoid confusion, we only show surface winds and simulated reactive aromatics over Tibet as in Fig. 5 in the paper.

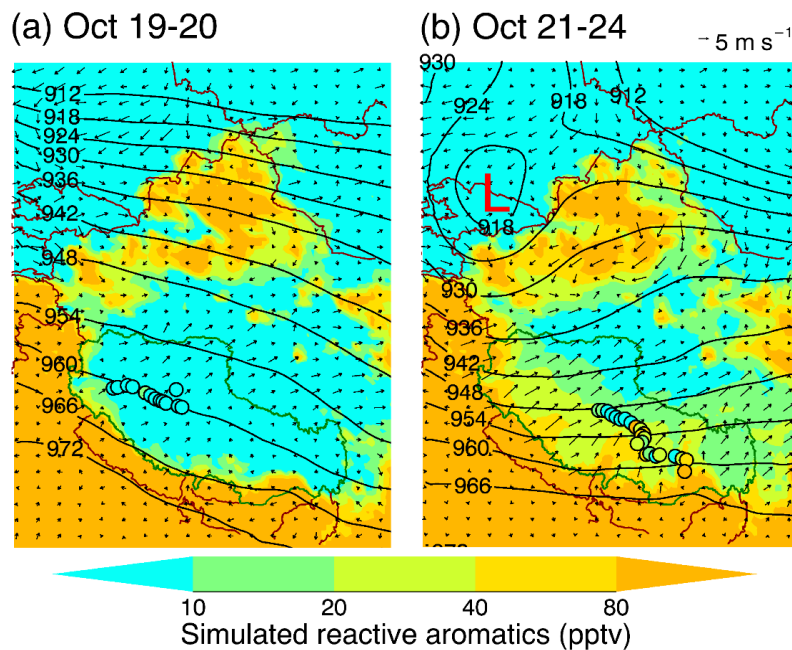


Figure AR1: Distributions of WRF simulated surface wind and REAM simulated concentrations of reactive aromatics over the Tibetan Plateau during October 19-20, 2010 (a) and October 21-24, 2010 (b). Circles show the observed reactive aromatics concentrations. Composite distributions of simulated reactive aromatics concentrations and surface wind, corresponding to sampling time of the observations, are shown in color and by arrows, respectively. Corresponding WRF simulated 300 hPa

geopotential height fields are shown by contour lines. The border of Tibet Autonomous Region is colored green.

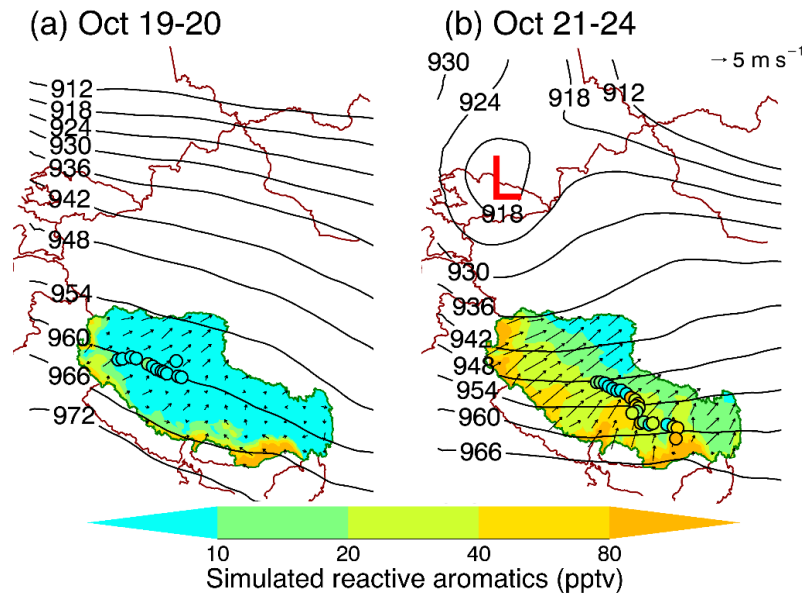


Figure 5: Distributions of WRF simulated surface wind and REAM simulated concentrations of reactive aromatics over the Tibetan Plateau during October 19-20, 2010 (a) and October 21-24, 2010 (b). Circles show the observed reactive aromatics concentrations. Composite distributions of simulated reactive aromatics concentrations and surface wind over Tibet, corresponding to sampling time of the observations, are shown in color and by arrows, respectively. Corresponding WRF simulated 300 hPa geopotential height fields are shown by contour lines. The border of Tibet Autonomous Region is colored green.

Technical Comments:

1. Page 1, Line 16: verb agreement: Long-range transport followed by deposition of black carbon on glaciers of Tibet is one of the key issues

Revised as suggested.

2. Page 1, Line 17: impacting the melting of glaciers

Corrected.

3. Page 1, Line 28: Remove “Furthermore”

Revised as suggested.

4. Page 2, Line 2: The Menon et al. (2002) paper should be cited.

Reference added.

5. Page 2, Line 5: Insert “altitude” or “surface elevation” after “4 km”

Corrected.

6. Page 2, Line 14 is an orphan sentence and is not really needed.

We moved this sentence.

7. Page 2, Line 19: “aerosols” may be a better word than “condensation nuclei”

Corrected.

8. Page 2, Line 20: “large-scale westerlies from East Asia” does not make sense. East Asia is east of Tibet, so it must be an easterly wind if the air moves east to west.

Corrected, it should be South Asia instead of East Asia.

9. Page 3, Line 20: Shouldn't Fig. 1a be cited before Fig. 1b?

Corrected.

10. Page 3, Line 23: I think it should be “overpass time” and not “overpassing”.

Corrected.

11. Page 4, Lines 4-8: Are all these references needed? It is sufficient to just cite 1-2 example references per topic.

These previous applications are relevant since they provide observation-based evaluations and applications to the REAM model. Successful applications in various environments demonstrate the capability of the model.

12. Page 4, Line 24: It would be good to cite Figure S1a.

We cite Fig. S3a (previously Fig. S1) in Section 2.4.

13. Page 5, Lines 2-4 is a long sentence. Please break it up into 2 sentences.

Revised as suggested.

14. Page 5, Line 2: I think it should be “overpass time” and not “overpassing”.

Revised as suggested.

15. Page 5, Line 28: I think it should be “overpass time” and not “overpassing”.

Revised as suggested.

16. Page 5, Line 29: Insert “did” before “for eastern China”.

Corrected.

17. Page 7, Line 15: I would suggest using “promote” instead of “provide”.

Revised as suggested.

18. Page 7, Line 24: Are the histograms for wind speed for at the surface (or 10-m winds)? Please clarify.

The histograms are for surface winds. We now clarify in the paper.

“Fig. 7 shows the histograms of observed and simulated surface wind speed for the 3 periods.”

19. References: Could the references be written so that they are easier to read? Either adding a “hanging indent” or a line space between references would help immensely.

Corrected, we now added a “hanging intent” for each reference.

20. Figure 4b: The black and dark blue colors are quite similar. Could a different color

be plotted?

We now used red and blue colors as suggested.

21. Figure S3: To emphasize the differences between the panels, it may be better to plot using the same scaling. The gradients can still be appreciated if a “log type” scaling is used, e.g. 1, 2, 3, 5, 7, 10.

We revised Fig. S4 (previously Fig. S3) as suggested.

22. Figure S7: The legend mistypes “original”. The original winds line does not look like the black line in Figure S4d.

The legend has been corrected. Black line in Fig. S10 (previously Fig. S7) shows ground-1km air mass fluxes during Period 1. Fig. S5d (previously Fig. S4d) shows ground-1km air mass fluxes during October 19-20 and October 21-24.

Response to Referee #2:

First of all, the Authors claim that their analysis has implications for improving the modelling of black carbon (BC) transport to the glaciated regions of Tibet (all the Introduction is dedicated to this topic). However, their approach is based on measurements (in situ and satellite retrievals) of aromatic HCs and of their degradation products (glyoxal). It is certainly true that aromatic hydrocarbons share with BC several emission and transport patterns, but only to a certain extent. For instance, the aromatic HCs are emitted by fossil fuel combustion, gasoline evaporation and solvent use (page 2, line 24), however only the first of these three sectors is of importance for BC. It follows that top-down methods for correcting the emissions of aromatic HCs (Section 2.4) has unclear implications for improving the representation of BC sources in the models. If the scope of the paper is really improving BC modelling in the Himalayan-Tibetan region, then the absence of BC observations poses a major caveat, even if the approach is conceptually valid and in principle it could be extended to experiments involving real BC measurements.

The implications of this paper for BC are only on transport. As the reviewer pointed out that our work cannot directly address the accuracy of BC emission inventories, which we did not claim in the paper that we can either. We suggest that aromatics observations are good proxies for understanding transport processes of BC to the Tibetan Plateau. The major pathway of transport is driven by the presence of a cut-off low system. Section 2.4 shows that the underestimates of aromatics transport are due to an underestimation of emissions, which can be improved using satellite observations.

To further demonstrate the link between transport of aromatics and BC to Tibet, we redistributed the total aromatics emissions over China and other South Asia countries on the basis the BC emission distributions. Therefore, the resulting aromatics emission distributions resembles that of BC. We conducted a sensitivity simulation using these emissions and compared the results to the original REAM simulation (Fig. S7). Transport of BC from South Asia (e.g., India) clearly dominates and it is strongly affected by the presence of a cut-off low system, as we discussed in the paper.

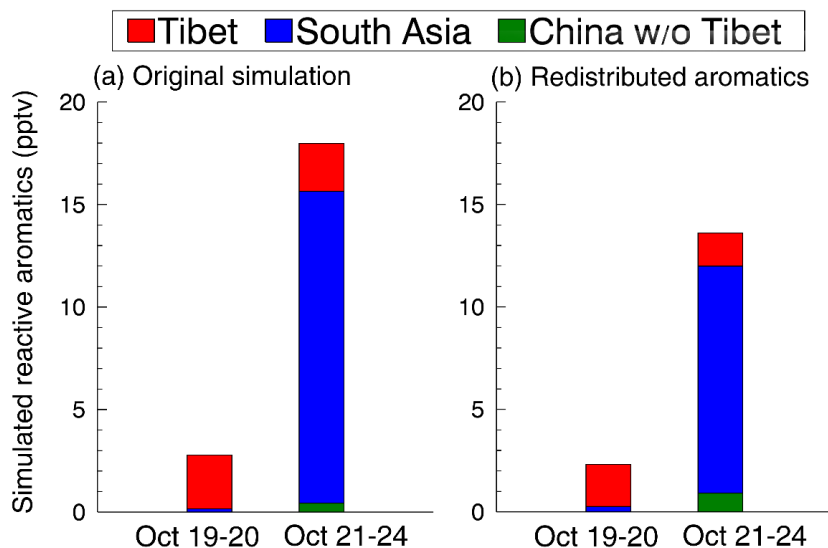


Figure S7: Averages of simulated reactive aromatics emitted from Tibet (red), India and nearby countries (“South Asia”, blue) and China excluding Tibet (“China w/o Tibet”, green) corresponding to in situ observations during October 19-20 and October 21-24. REAM simulations are conducted with original emissions (a) and the aromatics emissions redistributed following the BC emission distribution (b), respectively.

We now discuss this as well as the effects of BC wet deposition in Section 3.3.

“Compared to aromatics, BC is also subject to wet scavenging, which greatly reduces its transport efficiency by convection. During our analysis period, the cut-off low system and the associated precipitation are to the northwest of Tibet (Fig. S6 in the Supplement). Precipitation south of Tibet is weak and thus the subsequent removal of BC during trans-Himalaya transport is limited.

To examine the sensitivity of trans-Himalaya transport to the distribution of emission sources, we redistribute INTEX-B the total aromatics emissions over China and other South Asia countries on the basis of the MIX BC emission distributions. We conduct a sensitivity simulation using the redistributed emissions and compared the results to the original simulation. The trans-Himalaya transport from South Asia clearly dominates and it is strongly affected by the presence of a cut-off low system during our analysis period (Fig. S7 in the Supplement). Our analysis implies that BC transported in the presence of an upper tropospheric cut-off low is potentially a major contributor to BC deposition to Tibetan glaciers.”

Specific comments: a. Biomass burning is ruled out from the possible explanations for the difference between observed and retrieved glyoxal concentrations over the IGP, because satellite fire counts show only spot fire occurrence over the Plain with little correspondence with the model-measurement gap (Page 5, lines 10 – 14). However, open burning accounts for only a fraction of biomass burning, which is normally practiced also indoor for cooking, heating etc., undetected by remote sensing. Therefore, I would not rule out the hypothesis of a direct emission of glyoxal from domestic biomass burning.

We calculate indoor burning glyoxal emissions using emission factors from Pettersson et al. (2011) and Li et al. (2014). The Indian rural and urban population distribution from the NASA Socioeconomic Data and Applications Center (SEDAC) Network for year 2010 is used as spatial proxies. We adopt the energy consumptions for rural and urban inhabitants on the basis of the National Sample Survey Office of India (N.S.S.O., 2012a, 2012b). Simulated indoor burning contribution (Fig. S3) to glyoxal VCDs is lower by a factor of about 15 than the glyoxal VCDs discrepancy between satellite retrieval and model simulation. The uncertainty of the indoor energy consumption glyoxal emissions mainly results from the uncertainty of the emission factor. Even we assume this uncertainty to be 300%, indoor burning cannot explain the low bias of the simulated glyoxal VCDs. Thus, we consider that the underestimation of aromatics emissions is the main reason for the glyoxal VCD discrepancy. After accounting for model transport biases, the comparison of the model simulations using a priori emissions to in situ observations of reactive aromatics suggests that aromatics emissions in South Asia are underestimated.

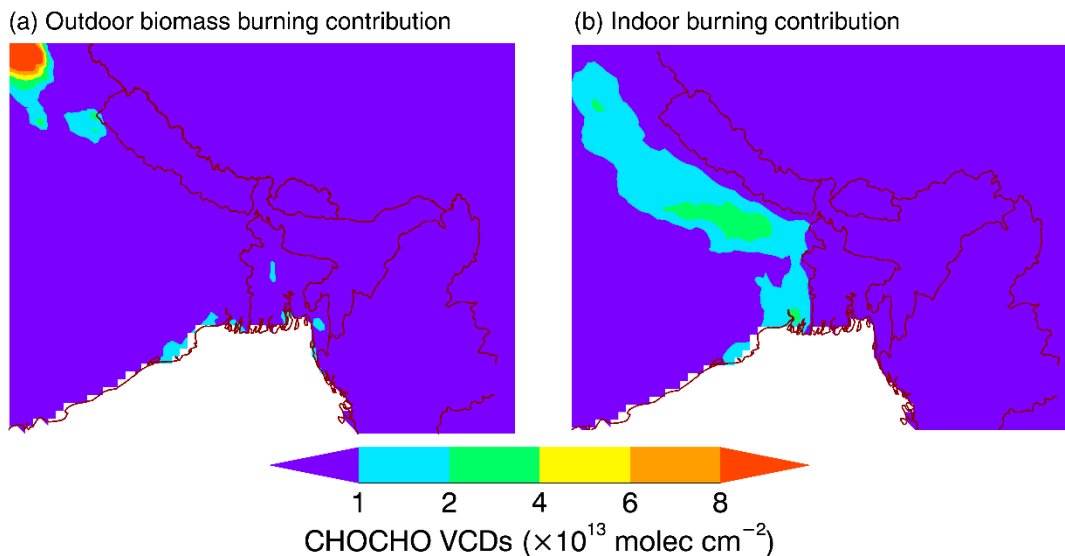


Figure S3: Contributions to CHOCHO VCDs from outdoor biomass burning (a) and indoor burning (b) emissions for October 2010.

We now discuss this in Section 2.3 and Section 2.4.

Section 2.3:

“Biogenic VOC emissions are computed with the Model of Emissions of Gases and Aerosols from Nature (MEGAN) algorithm (v2.1, Guenther et al., 2012) and outdoor biomass burning emissions of CHOCHO and other species are based on Global Fire Emissions Database Version 4.1 with small fires (GFED4.1s, van der Werf et al., 2010; Andreae and Merlet, 2001; Lerot et al., 2010). Indoor burning CHOCHO emissions of India are computed using emission factors from Pettersson et al. (2011) and Li et al. (2014). Rural and urban population distributions of India for year 2010 are used as spatial proxies (Balk et al., 2006; CIESIN, 2011, 2016). We adopt the energy consumptions for rural and urban inhabitants on the basis of the National Sample Survey Office of India (N.S.S.O., 2012a, 2012b).”

Section 2.4:

“~~The distribution of localized contribution to~~ CHOCHO emissions VCDs from outdoor biomass burning (Fig. ~~S4S3a in the~~ Supplement) differs greatly from that of ΔC_{CHOCHO} (Fig. ~~S2a in Supplement 2c~~), which is large over the industrialized Indo-Gangetic Plain. Simulated indoor burning contribution to CHOCHO VCDs is lower by a factor of about 15 than the CHOCHO VCDs discrepancy between satellite retrieval and model simulation (Fig. S3b in the Supplement). The uncertainty of the indoor burning CHOCHO emissions mainly results from that of the emission factor. Even we assume this uncertainty to be 300%, indoor burning cannot explain the low bias of the simulated CHOCHO VCDs. Therefore, it is considered that the large model underestimation of CHOCHO over the Indo-Gangetic Plain is unlikely due to outdoor biomass burning or indoor burning during our analysis period.”

b. The Authors find a plausible explanation for the rise of aromatic HCs concentrations between 22 and 24 Oct 2010 in the synoptic meteorological conditions in central Asia showing an upper-level cut-off system triggering a southerly circulation from India to Tibet. However, minding that BC can be removed during transport by precipitations, the Authors should provide a more in-depth analysis of the meteorological conditions over the Himalayans during the approach of the low-pressure system. Apparently, on the 22 of

October, frontal cloud systems travelled over the Tibet from west to east (<http://www.ssec.wisc.edu/data/comp/ir/2010295M0000.gif>). The presence of precipitations with possible losses of BC (and not necessarily of aromatic HCs) in the Himalayas should be checked carefully at local meteorological stations.

This is a good point for BC concentration distribution over the Tibet, which is not studied in this work. Our focus is on transport. BC still needs to be transported to the Tibetan region; scavenging can only reduce the BC amount. If BC is not transported to the region in the first place, scavenging cannot increase BC in this region.

Our study suggests that the cut-off low system is difficult to simulate with a regional model constrained by meteorological observations. It would be much harder for climate models to simulate correctly. Fig. S6 in the Supplement shows the precipitation distribution for October 19-20 and October 21-24. The cut-off system is to the northwest of Tibet. Precipitation south of the Himalayas is weak and hence the removed BC from precipitation during the trans-Himalaya transport is limited.

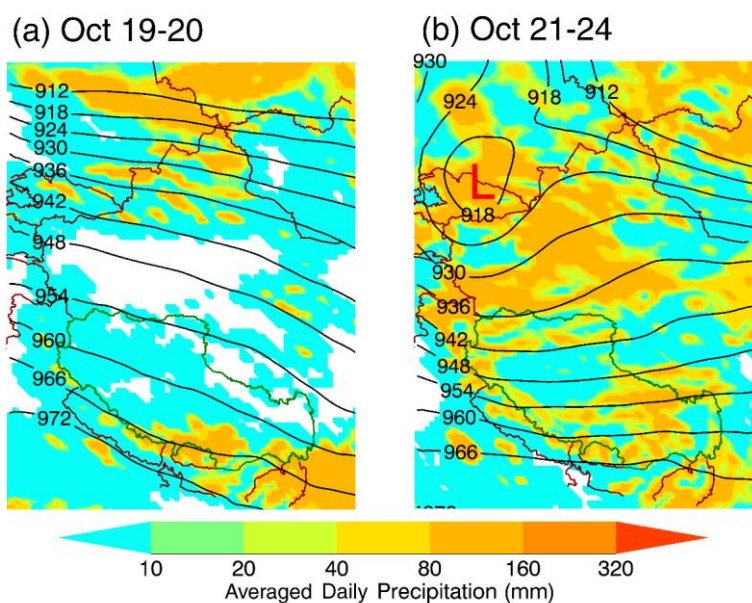


Figure S6: WRF simulated averaged daily precipitation for October 19-20 (a) and October 21-24 (b), respectively.

We now discuss the related issues in Section 3.3.

“Accompanying this transport, large amounts of pollutants such as reactive aromatics analyzed here are transported to the Tibetan Plateau leading to much higher surface concentrations.

The cut-off low system provides a more rapid and efficient pollutants transport pathway compared with transport pathways previously proposed by other studies, such as westerlies (Cong et al., 2015; Ji et al., 2015) and mountain-valley winds (Hindman and Upadhyay 2002; Dumka et al., 2010). Compared to aromatics, BC is also subject to wet scavenging, which greatly reduces its transport efficiency by convection. During our analysis period, the cut-off low system and the associated precipitation are to the northwest of Tibet (Fig. S6 in the Supplement). Precipitation south of Tibet is weak and thus the subsequent removal of BC during trans-Himalaya transport is limited.”

Enhanced Trans-Himalaya Pollution Transport to the Tibetan Plateau by the Cut-off Low System

Ruixiong Zhang¹, Yuhang Wang¹, Qiusheng He², Laiguo Chen³, Yuzhong Zhang¹, Hang Qu¹, Charles Smeltzer¹, Jianfeng Li¹, Leonardo M.A. Alvarado⁴, Mihalis Vrekoussis^{4,5,6}, Andreas Richter⁴, Folkard Wittrock⁴, and John P. Burrows⁴

¹School of Earth and Atmospheric Sciences, Georgia Institute of Technology, Atlanta, GA

²School of Environment and Safety, Taiyuan University of Science and Technology, Taiyuan, China

³Urban Environment and Ecology Research Center, South China Institute of Environmental Sciences (SCIES), Ministry of Environmental Protection (MEP), Guangzhou, China

⁴Institute of Environmental Physics and Remote Sensing, University of Bremen, Bremen, Germany

⁵Center of Marine Environmental Sciences – MARUM, University of Bremen, Germany

⁶Energy, Environment and Water Research Center (EEWRC), The Cyprus Institute, Nicosia, Cyprus

Correspondence to: Yuhang Wang (ywang@eas.gatech.edu), Qiusheng He (heqs@tyust.edu.cn)

Abstract. Long-range transport ~~and subsequent~~followed by deposition of black carbon on glaciers of Tibet is one of the key issues of climate research inducing changes on radiative forcing and subsequently impacting ~~on~~ the melting of glaciers. The transport mechanism, however, is not well understood. In this study, we use short-lived reactive aromatics as proxies to diagnose transport of pollutants to Tibet. In situ observations of short-lived reactive aromatics across the Tibetan Plateau are analyzed using a regional chemistry and transport model. The model performance using the current emission inventories over the region is poor due to problems in the inventories and model transport. Top-down emissions constrained by satellite observations of glyoxal (~~CHOCHO~~) are a factor of 2-6 higher than the a priori emissions over the industrialized Indo-Gangetic Plain. Using the top-down emissions, agreement between model simulations and surface observations of aromatics improves. We find enhancements of reactive aromatics over Tibet by a factor of 6 on average due to rapid transport from India and nearby regions during the presence of a high-altitude cut-off low system. Our results suggest that the cut-off low system is a major pathway for long-range transport of pollutants such as black carbon. The modeling analysis reveals that even the state-of-the-science high-resolution reanalysis cannot simulate this cut-off low system accurately, which probably explains in part the underestimation of black carbon deposition over Tibet in previous modeling studies. ~~Furthermore,~~ ~~another~~Another model deficiency of underestimating pollution transport from the south is due to the complexity of terrain, leading to enhanced transport. It is therefore challenging for coarse-resolution global climate models to properly represent the effects of long-range transport of pollutants on the Tibetan environment and the subsequent consequence for regional climate forcing.

1 Introduction

The Tibetan Plateau, commonly referred as the Third Pole and the last pristine land of the Earth, has drawn much attention in environmental and climate research in recent years- ([Menon et al., 2002](#)). Although Tibet appears to be isolated from industrialized regions due in part to the transport barrier by its being a plateau

and its pollutant concentrations being generally low, the Third Pole is vulnerable to regional climate change. Areas of the Tibetan Plateau over 4 km in altitude are warming at a rate of 0.3 °C per decade, twice as fast as the global average (Xu et al., 2009). In addition to the increase of greenhouse gases (GHGs) and the associated global warming, black carbon (BC) is likely another important contributor to the warming of the Tibetan Plateau. The deposition of BC on the vast glaciers of the Tibetan Plateau will decrease the surface albedo, accompanied by increased sunlight absorption and subsequent enhanced melting (Hansen and Nazarenko, 2004; Ramanathan and Carmichael, 2008; Ming et al., 2009; Yasunari et al., 2010). Increasing BC concentrations were previously found in ice core and lake sediment records (Xu et al., 2009; Cong et al., 2013). The dwindling of glaciers over Tibet is a major concern for fresh water supply to a large portion of the Asian population through the Indus River, Ganges River, Yarlung Tsangpo River, Yangtze River and Yellow River (Singh and Bengtsson, 2004; Barnett et al., 2005; Lutz et al., 2014). Though melting glaciers favor river runoff temporarily, mass loss of glaciers endangers water supply during the dry season in the future (Yao et al., 2004; Kehrwald et al., 2008).

~~Increasing BC concentrations were already found in ice core and lake sediment records (Xu et al., 2009; Cong et al., 2013)~~. Besides narrowing the uncertainties of BC emissions, aging and deposition, better understanding the transport pathways are equally important in this region. Surrounded by the largest ~~black carbon~~ BC sources of East Asia and South Asia (Bond et al., 2007; Ohara et al., 2007), Tibet is primarily affected by pollutant transport from these two regions (Kopacz et al., 2011; Lu et al., 2012; Zhao et al., 2013; Wang et al., 2015; Zhang et al., 2015); Li et al., 2016; Wang et al., 2016; Kang et al., 2016). Kopacz et al. (2011) attempted to identify the sources of BC over glaciers in the Himalayas and the Tibetan Plateau (HTP) using the adjoint model of GEOS-Chem. Lu et al. (2012) developed a novel back-trajectory model with BC emissions, hydrophilic-to-hydrophobic aging, and deposition and found that South Asia and East Asia account for 67% and 17% of BC over the HTP. Using source tagging, biofuel and biomass burning emissions from South Asia are found to be the largest sources of BC in HTP followed by fossil fuel combustion emissions (Zhang et al., 2015). Hindman and Upadhyay (2002) ~~proposed~~ suggested that the vertical lifting due to convection and subsequent horizontal mountain-valley wind lead to the transport of ~~condensation nuclei~~ aerosols from Nepal to Tibet. ~~Cong et al.~~ Dumka et al. (2010) also stressed the importance role of mountain-valley wind in BC concentration in Central Himalayas. Cong et al. (2015) suggested that both the large-scale westerlies from EastSouth Asia and the local mountain-valley wind from South Asia are major transport pathways. The synoptic scale trough and ridge can potentially lead to the trespassing of atmospheric brown clouds from South Asia to the Tibetan Plateau (Lüthi et al., 2015). Ji et al. (2015) indicated that the southwesterlies during monsoon season favor aerosols transport across the Himalayas from South Asia. Aerosols observations in previous studies are mostly limited to the southern and northern slopes of the Himalayas (Hindman and Upadhyay, 2002; Dumka et al., 2010; Cong et al., 2015) with very few in situ sites (e.g. Namco, Linzhi) inside Tibet (Kopacz et al., 2011; Ji et al., 2015; Lüthi et al., 2015; Zhang et al., 2015). Considering the complex topography (Lawrence and Lelieveld, 2010; Ménégos et al., 2013; He et al., 2014; Kumar et al., 2015) and scarce observations (Maussion et al., 2011), it is crucial to evaluate model simulated

transport performance over the Tibetan Plateau using available observations with a good spatial coverage.

Observation-constrained modeling, ~~however~~, is needed to better understand potential model biases- due to the uncertainties of model simulated transport from South Asia to Tibet.

In this study, we use short-lived reactive aromatics as proxies to diagnose transport of pollutants to Tibet. In situ observations of short-lived reactive aromatics across the Tibetan Plateau are analyzed (Section 2.1). Anthropogenic emissions including fossil fuel combustion, gasoline evaporation and solvent use constitute the main ~~sources~~sources of atmospheric aromatics (Sack et al., 1992; Fu et al., 2008; Henze et al., 2008; Cagliari et al., 2010; Cabrera-Perez et al., 2016). Biofuel and biomass burning is another important source (Fu et al., 2008; Henze et al., 2008). The main sink of aromatics is OH oxidation with lifetimes ranging from hours to days (Atkinson, 2000; Liu et al., 2012b). We use satellite observations to minimize the biases of emission inventories for upwind regions of Tibet (Sections 2.2, 2.3 and 2.4) and then apply a regional chemistry and transport model constrained by high-resolution reanalysis meteorological data to understand missing transport processes in model simulations (Section 3). On the basis of these results, we examine the implications for global climate modeling studies of anthropogenically driven changes over the Tibetan Plateau (Section 4).

2 Methods

2.1 In situ aromatics data

Whole air samples were collected in 2-L electro-polished stainless-steel canisters, which had been cleaned and vacuumed according to the TO-15 method issued by US EPA before shipment to the sampling sites. The restricted grab sampler (39-RS-x; Entech), which has a 5- μ m Silonite-coated metal particulate filter, was placed on the inlet of the canister to completely filter out dust and other particulates during sampling. These samples were taken in daytime from 8:00 AM to 7:00 PM with an interval of 1 to 2 hours. The sampling time was 5 minutes to fill the vacuumed canisters. The filled canisters were transported back to the laboratory of Guangzhou Institute of Geochemistry, Chinese Academy of Science. Each air sample was analyzed for 65 light non-methane hydrocarbons (NMHCs) species. The samples were pretreated by an Entech Model 7100 Preconcentrator (Entech Instruments Inc., California, USA), and analyzed by a gas chromatography-mass selective detector (GC-MSD/FID, Agilent 7890A/5973N, USA) using dual columns and dual detectors to simultaneously analyze both low- and high-boiling-point VOCs with each injection. The detailed analytical procedure is described by Zhang et al. (2012).

In this study, we analyze 65 measurements of aromatics (benzene, toluene, ethyl-benzene, m/p/o-xylene) and wind speed measurements taken across Tibet during October 2010 (Fig. ~~4b1a~~4b1a). Care was taken in sampling such that there are no direct urban, industrial, or road emissions in the upwind direction of the sampling location. The lifetimes of toluene, ethyl-benzene, m/p/o-xylene are relatively short (2-20 hours) and these reactive aromatic compounds therefore provide observational constraints for transport from India and nearby regions to Tibet. We group the samples into three periods based on the time and locations of the

measurements, i.e. Period 1 from October 13 to 17, 2010 to the north of the Himalayas along the southern border of Tibet, Period 2 from October 19 to 24 across the interior of the Tibetan Plateau, and Period 3 of October 25 to the Westwest of the Yarlung Tsangpo Grand Canyon in southeastern Tibet (Fig. 4b1a).

2.2 SCIAMACHY CHOCHO measurements

The SCanning Imaging Absorption spectroMeter for Atmospheric CHartographY (SCIAMACHY) onboard Environmental Satellite (ENVISAT) operated from 2002 to 2012 (Burrows et al., 1995, Bovensmann et al., 1999), with an overpassingoverpass time at about 10:00 AM local time. SCIAMACHY made passive remote sensing measurements of the upwelling radiation from the top of the atmosphere in alternate nadir and limb viewing geometry. Mathematical inversion of the measurements of SCIAMACHY yields a variety of data products including glyoxal (CHOCHO) Vertical Column Densities (VCDs, unit: *molecules cm⁻²*). The retrieval uses the Differential Optical Absorption Spectroscopy (DOAS) technique (Wittrock et al., 2006; Vrekoussis et al., 2009; Alvarado et al., 2014). The CHOCHO retrieval used in this study is based on the algorithm developed in Alvarado et al. (2014), which includes corrections for the interferences with nitrogen dioxide (NO₂) over the regions with high NO_x emissions as well as liquid water over oceans (Alvarado, 2016). Detection limit for SCIAMACHY CHOCHO VCD is about 1×10^{14} *molecules cm⁻²*. The overall monthly uncertainty of CHOCHO VCDs ($\frac{C_{CHOCHO}^{observed}}{C_{CHOCHO}^{SCIAMACHY}}$) in the selected region during October 2010 is given by $\alpha \times \frac{C_{CHOCHO}^{observed}}{C_{CHOCHO}^{SCIAMACHY}} \times C_{CHOCHO}^{SCIAMACHY} + 1 \times 10^{14}$ *molecules cm⁻²*, where the value of α is in a range of 0.1 to 0.3. Following the method as described by Liu et al. (2012b), we derive a top-down aromatics emission estimate for South Asia constrained by CHOCHO retrievals described in Section 2.4.

2.3 3-D REAM model

We use the 3-D Regional chEmical trAnsport Model (REAM) to examine the chemistry evolution and regional transport of aromatics. REAM was used in previous studies, including large-scale transport (Wang et al., 2006; Zhao et al., 2009b, 2010), vertical transport (Zhao et al., 2009a; Zhang et al., 2014, 2016), emission estimates (Zhao and Wang, 2009; Liu et al., 2012b; Gu et al., 2013, 2014, 2016) and other air quality studies (Zeng et al., 2003, 2006; Choi et al., 2005, 2008a, 2008b; Wang et al., 2007; Liu et al., 2010, 2012a, 2014; Gray et al., 2011; Yang et al., 2011; Zhang and Wang, 2016).

REAM has a horizontal resolution of 36 km with 30 vertical levels in the troposphere and 5 vertical levels in the stratosphere covering adjacent regions of China (Fig. 4a1b). The model top is at 10 hpa. Meteorological fields in REAM are obtained from the Weather Research and Forecasting model (WRF) assimilations constrained by National Centers for Environmental Prediction Climate Forecast System Reanalysis (NCEP CFSR, Saha et al., 2010) 6-hourly products, which have a horizontal resolution of T382 (~38 km). We run the WRF model with the same resolution as in REAM with a domain ~~is~~ larger than that of REAM by 10 grid cells on each side. Meteorological inputs related to convective transport are updated every 5 minutes while the others are updated every 30 minutes. The recent update of REAM expands the GEOS-Chem standard chemical mechanism (V9-02) to include a detailed description of ~~aromatic~~aromatics chemistry (Bey et al.,

2001; Liu et al., 2010, 2012b). Aromatics are lumped into three species based on reactivity, i.e. ARO1 (toluene, ethyl-benzene), ARO2 (m/p/o-xylene), and benzene. The atmospheric lifetimes of the three aromatics tracers against OH are 18 hours, 4.2 hours and 3.9 days during the study period (October 13-25, 2010), respectively. Due to the long atmospheric lifetime of benzene, it is more difficult to track and identify its sources; thus we do not explicitly discuss benzene in this study. We focus our analysis on reactive aromatics (toluene, ethyl-benzene, and m/p/o-xylene).

~~Meteorological fields in REAM are obtained from the Weather Research and Forecasting model (WRF) assimilation constrained by National Centers for Environmental Prediction Climate Forecast System Reanalysis (NCEP-CFSR, Saha et al., 2010). CFSR has a horizontal resolution of T382 (~38 km). Initial and boundary conditions for chemical tracers are taken from GEOS-Chem (V9-02) 2° × 2.5° simulation- (Bey et al., 2001). Anthropogenic emissions in China and other Asian countries are from the are from the MIX inventory for October 2010 (Li et al., 2015). MIX is a mosaic Asian anthropogenic emission inventory with the Multi-resolution Emission Inventory for China (MEIC v1.0) for 2010 and updated-) for China and several other emission inventories for other Asian countries. In addition to the MIX inventory, we also conduct sensitivity simulations using the Intercontinental Chemical Transport Experiment-Phase B (INTEX-B) emission for 2006 (emissions inventory (Zhang et al., 2009; Li et al., 2014), respectively- which was developed for the year 2006. We find that compared to the in situ observations of aromatics, the simulation results using the INTEX-B emissions are better. The main reason for the simulation improvements is due to the emissions of aromatics in South Asia. Given the large uncertainties in the emissions of aromatics (e.g., Liu et al., 2012b), this result is not surprising. Since MEIC and INTEX-B inventories are developed by the same group, we replace MIX aromatics emissions outside China with INTEX-B data such that aromatics emissions in the model are consistent. The improvements of model simulations compared to in situ observations are shown in Fig. S1 in the Supplement. Since satellite observations are used to improve aromatics emissions (next section), using either MIX or INTEX-B emissions in this work gives the same conclusions.~~ Biogenic VOC emissions are computed with the Model of Emissions of Gases and Aerosols from Nature (MEGAN) algorithm (v2.1, Guenther et al., 2012) and outdoor biomass burning emissions of CHOCHO and other species are based on Global Fire Emissions Database Version 4.1 with small fires (GFED4.1s, van der Werf et al., 2010; Andreae and Merlet, 2001; Lerot et al., 2010). Indoor burning CHOCHO emissions of India are computed using emission factors from Pettersson et al. (2011) and Li et al. (2014). Rural and urban population distributions of India for year 2010 are used as spatial proxies (Balk et al., 2006; CIESIN, 2011, 2016). We adopt the energy consumptions for rural and urban inhabitants on the basis of the National Sample Survey Office of India (N.S.S.O., 2012a, 2012b). Compared with satellite observed CO and NO₂ VCDs, REAM performs reasonably well in the study region during October 2010 (Fig. S2 in the Supplement). For general model evaluations of REAM, we refer the readers to the papers cited early in this section.

We updated the INTEX-~~B~~ emission inventory in South Asian countries through inverse modeling constrained by SCIAMACHY CHOCHO VCDs (Section 2.4next section). We run REAM simulations with

the a priori and top-down emission inventories, and compare the results with observations in Section 3.1 and 3.2, respectively. We find that some of the model low bias is likely due to emission underestimation. We further carried out three model sensitivity tests to calculate the contributions to surface aromatics from emissions over Tibet, other provinces of China, and South Asia (India and nearby regions). Each simulation is run with only the aromatics emissions from the corresponding region. The OH concentrations in each simulation are specified to the archived values of the full model simulation. The results for two sub-periods of Period 2 are examined in Section 3.3.

2.4 Top-down aromatics emission estimation

Compared with SCIAMACHY data, REAM using the original emission inventories archived at the ~~overpassing~~ time of SCIAMACHY underestimates CHOCHO VCDs in the populated regions of India (Fig. 2). This underestimation is especially significant in the Indo-Gangetic Plain located south of the Himalayas. (Fig. 2c). We then derive the top-down aromatics emissions for these regions constrained by SCIAMACHY CHOCHO data (Liu et al., 2012b; Alvarado, 2016).

First, we calculate the difference between observed ($C_{CHOCHO}^{SCIAMACHY}$, Fig. 2a) and modeled (C_{CHOCHO}^{REAM} , Fig. 2b) CHOCHO VCDs with original emissions ($\Delta C_{CHOCHO} = C_{CHOCHO}^{SCIAMACHY} - C_{CHOCHO}^{REAM}$, Fig. ~~S2a in Supplement~~ 2c). This discrepancy greatly exceeds the uncertainties of SCIAMACHY retrieval. We then discuss the potential reasons for the difference, i.e. primary emissions from biomass burning and secondary sources from isoprene, acetylene, ethylene and aromatics. (Fu et al., 2008; Liu et al., 2012b).

Biomass burning is often a major primary source of CHOCHO (Myriokefalitakis et al., 2008). GFED4.1s inventories, as well as fire hotspots observed by MODIS on board the Terra and Aqua satellites, indicate only a small number of fire occurrences during this period in South Asia, with the exception of crop residue burning in Punjab, an agricultural state in North India. The ~~distribution of localized~~ contribution to CHOCHO ~~emissions~~ VCDs from outdoor biomass burning (Fig. ~~S+S3a in the Supplement~~) differs greatly from that of ΔC_{CHOCHO} (Fig. ~~S2a in Supplement~~ 2c), which is large over the industrialized Indo-Gangetic Plain. Simulated indoor burning contribution to CHOCHO VCDs is lower by a factor of about 15 than the CHOCHO VCDs discrepancy between satellite retrieval and model simulation (Fig. S3b in the Supplement). The uncertainty of the indoor burning CHOCHO emissions mainly results from that of the emission factor. Even we assume this uncertainty to be 300%, indoor burning cannot explain the low bias of the simulated CHOCHO VCDs. Therefore, ~~it is considered that~~ the large model underestimation of CHOCHO over the Indo-Gangetic Plain is unlikely due to outdoor biomass burning or indoor burning during our analysis period.

Direct anthropogenic emissions of CHOCHO are small (Volkamer et al., 2005; Stavrou et al., 2009; Liu et al., ~~2012-b~~ 2012b). CHOCHO is produced primarily from the photochemical oxidation of biogenic compounds (e.g., isoprene and terpenes) and hydrocarbon released by anthropogenic activities (e.g., acetylene, ethylene, and aromatics) (Fu et al., 2008). Due to the long atmospheric lifetime of acetylene and ethylene, their contributions to CHOCHO concentrations are quite small in South Asia during October 2010. The most significant secondary sources of CHOCHO in South Asia are isoprene (Fig. ~~S2b in Supplement~~ 2d)

and aromatics (Fig. ~~S2c in Supplement 2e~~). Biogenic isoprene emissions depend on vegetation, sunlight, and temperature. ~~High~~The high isoprene ~~emissions are~~contribution to CHOCHO VCDs is to the southeast of the Indo-Gangetic Plain, where CHOCHO VCDs are high in both the observations and model simulations. In comparison, aromatics oxidation dominates CHOCHO over the Indo-Gangetic Plain, where model underestimation is largest (Fig. ~~2 and Fig. S2 in Supplement 2~~).

We apply the approach by Liu et al. (2012b) to estimate the top-down emissions of aromatics based on SCIAMACHY CHOCHO VCDs. As found by Liu et al. (2012b), domain-wide inversion is impractical since model results correlate poorly with gridded satellite data, most likely reflecting the problems in the spatial distribution of a priori emissions. We therefore determine the emissions by inversion for each grid cell at the ~~overpassing~~overpass time of SCIAMACHY as Liu et al. (2012b) and find similar results for India and nearby regions as Liu et al. (2012b) ~~did~~ for eastern China. The top-down biogenic isoprene emissions are essentially the same as the a priori emissions. However, the top-down anthropogenic emissions of aromatics (Fig. ~~S3b~~S4 in ~~the~~ Supplement) increase by a factor of 2-6. The improved model comparison with in situ observations will be discussed in the next section. One caveat with respect to the top-down emission estimate is that we have to assume that the speciation of aromatics in the a priori emission inventory is correct. Since the purpose of this work is to study transport pathways to the Tibetan Plateau on the basis of in situ observations, we examine lumped reactive aromatics (defined as the sum of toluene, ethyl-benzene, and m/p/o-xylene) in the model evaluation (Section 3.2). Satellite observations cannot be used for this purpose since CHOCHO VCDs over Tibet are below or around the detection limit.

3 Results and discussion

3.1 Observed and simulated reactive aromatics

The average of observed reactive aromatics surface concentration (59 ± 63 pptv) over the Tibetan Plateau is considerably lower than the values found for megacities of China, such as Beijing (8.04 ppbv) and Shanghai (5.2 ppbv) (Liu et al., 2012b). Higher aromatics levels were measured during Period 1 (76 ± 39 pptv) and Period 3 (169 ± 57 pptv) than in Period 2 (26 ± 39 pptv). The model simulation using the a priori emissions in general compares poorly with the in situ observations (Fig. 3). The best performance is during the low-concentration Period 2 when the model underestimates the observations by about a factor of 2. However, the relatively high correlation coefficient ($R^2=0.8883$) suggests that atmospheric transport and emission distribution are reasonably simulated. This is in sharp contrast to Periods 1 and 3 when the model underestimates the observations by a factor of 5-7 with ~~no or~~ very low correlations between ~~the~~ model and the observations (slope= 0.2414 and 0.15 , $R^2=0.0004$ and 0.02 for Period 1 and 3, respectively). We discuss the different reasons for the model performance for Period 1, 2 and 3 in the next 3 sections.

3.2 Improvements due to top-down emissions

Fig. 2 and Fig. S3S4 in the Supplement show that SCIAMACHY observations of CHOCHO suggest much higher industrial emissions of aromatics over the Indo-Gangetic Plain than the a priori emissions. We derive top-down emissions on the basis of SCIAMACHY CHOCHO VCDs (Section 2.4). Top-down emissions are higher than the a priori emissions by a factor of 2-6 over the Indo-Gangetic Plain, which is the upwind region of the Tibetan Plateau. Fig. 4 shows the resulting improvement in the model simulation. The large underestimations of CHOCHO ~~VCDs~~VCDs over the Indo-Gangetic Plain are corrected as expected (Fig. 4a). At the same time, in situ observations during Period 2 are much better reproduced by the model with the slope increasing from 0.6256 to 0.9591 and a similar R^2 value (0.8066) (Fig. 4b). In contrast, model simulations for Periods 1 and 3 are not improved using top-down emission estimates with low biases similar to the original model simulation. This indicates that the reasons for the discrepancies in Periods 1 and 3 are probably not related to the uncertainties in emissions but could be linked to deficiencies in model transport in this area.

3.3 Rapid trans-Himalaya transport due to a high-level cut-off Low System

Observed and simulated reactive aromatics concentrations show large ~~variability~~variabilities during Period 2 (Fig. 4b). An investigation of these data shows that a major contributor is meteorology. Observed concentrations of reactive aromatics during October 19-20 are generally lower (6.6 ± 3.4 pptv), in comparison to those during October 21-24 (37 ± 45 pptv). The concentration difference during the two time periods is captured by model simulations with top-down emissions (Fig. 5). Analysis of WRF simulated surface wind speed shows an increase by a factor of 2-4 from October 19-20 (Fig. 5a) to 21-24 (Fig. 5b), corresponding well to increasing transport of aromatics from the Indo-Gangetic Plain.

To further analyze the difference between the two time periods, we conduct sensitivity simulations ~~in which OH concentrations in the model are specified to the archived values of the full model simulation using top-down emissions as described in Section 2.3.~~ We compute the source attributions for emissions over Tibet, India and nearby regions, and China excluding Tibet (Fig. 6). During October 19-20, reactive aromatics are due to Tibetan emissions. With the exception of one data point, ~~the~~ concentrations are ≤ 7 pptv. On October 21, emissions from India and nearby regions become dominant while the concentrations are still low (~~7-18~~21 pptv). During October 22-24, however, emissions from India and nearby regions contribute much higher concentrations (~~12-128~~10-137 pptv). The only exception is one data point sampled at 30 km east of Lhasa, where ~~most~~about one fifth of the population of Tibet resides. The contribution by emissions of India and nearby regions to this data point is ~ 20 pptv, still much higher than during October 19-20. The contribution by emissions from China (excluding Tibet) is negligible ($\sim 1\%$) for this period.

The rise of the Tibetan Plateau is a natural barrier for pollution transport (Fig. 1). Considering the high altitude of the Tibetan Plateau, we analyze 300 hPa geopotential height field in order to understand the change of wind circulation over the region (Fig. 5). During October 19-20, the upper troposphere shows a northward gradual pressure decrease, which does not ~~provide~~promote near-surface forcing of trans-Himalaya transport

(Fig. 5a). During October 21-24, the presence of a southeastward-moving upper tropospheric cut-off low system induces increasingly stronger surface wind from India to Tibet (Fig. 5b, Hoskins et al., 1985). The cut-off low system is a closed low-pressure system detached from the westerlies. It began to form on October 21 and started to dissipate on October 24. Trans-Himalaya air mass flux in the lower atmosphere shows an increase by a factor of 2 to 5 (Fig. S4S5 in the Supplement). Accompanying this transport, large amounts of pollutants such as reactive aromatics analyzed here are transported to the Tibetan Plateau leading to much higher surface concentrations.

The cut-off low system provides a more rapid and efficient pollutants transport pathway compared with transport pathways previously proposed by other studies, such as westerlies (Cong et al., 2015; Ji et al., 2015) and mountain-valley winds (Hindman and Upadhyay 2002; Dumka et al., 2010). Compared to aromatics, BC is also subject to wet scavenging, which greatly reduces its transport efficiency by convection. During our analysis period, the cut-off low system and the associated precipitation are to the northwest of Tibet (Fig. S6 in the Supplement). Precipitation south of Tibet is weak and thus the subsequent removal of BC during trans-Himalaya transport is limited.

To examine the sensitivity of trans-Himalaya transport to the distribution of emission sources, we redistribute INTEX-B the total aromatics emissions over China and other South Asia countries on the basis of the MIX BC emission distributions. We conduct a sensitivity simulation using the redistributed emissions and compared the results to the original simulation. The trans-Himalaya transport from South Asia clearly dominates and it is strongly affected by the presence of a cut-off low system during our analysis period (Fig. S7 in the Supplement). Our analysis implies that BC transported in the presence of an upper tropospheric cut-off low is potentially a major contributor to BC deposition to Tibetan glaciers.

3.4 Missing cut-off low system and complex terrain

Compared to Period 2, model performance for Periods 1 and 3 is very poor with severe low biases (Fig. 3). Transport deficiency appears to be the main problem. Fig. 7 shows the histograms of observed and simulated surface wind speed for the 3 periods. The observed and simulated wind speed distributions are similar for Period 2 (Fig. 7c). In comparison, the simulated wind speed distribution differs drastically for the other two periods (Fig. 7a and 7d).

The wind speed distributions are more similar between Period 1 and 2 in the observations than model simulations. The underestimation of wind speed in Period 1 leads to slower transport of pollutants from the Indo-Gangetic Plain and consequently to a low bias in surface reactive aromatics in the model. Examination of the 300 hPa geopotential height field during October 13-17 of Period 1 shows a weak trough northeast of Kazakhstan in CSFR reanalysis and WRF simulation results (Fig. S5S8 in the Supplement). A strong upper tropospheric low pressure system, akin to the cut-off low system of Fig. 5b, will induce stronger lower troposphere wind circulation. The lack of radiosonde observations over the interior of the Tibetan Plateau to constrain the meteorological reanalysis is the plausible reason (Fig. S6S9 in the Supplement). The horizontal scale of the Rossby Wave at northern mid latitudes is thousands of kilometers, which can be reasonably

represented by the density of the existing radiosonde network. We hypothesize that the smaller scale cut-off low system, not simulated in [the](#) reanalysis, is more likely the reason for the model-observation discrepancy during Period 1. We resample surface wind speed of October 23, when a cut-off low system leads to rapid trans-Himalaya transport in Period 2 analyzed in the previous section. At the same time of the day and location as the observations, the simulated wind speed histogram is in good agreement with the observations (Fig. 7b). The corresponding air mass flux across the Himalayas would have been much stronger in the presence of a cut-off low system (Fig. [S7S10](#) in [the](#) Supplement).

During Period 3, the observed wind speed histogram is skewed to very low wind speed (0-1 m/s) compared to the simulations (Fig. 7d). Sampling bias to avoid locations with strong wind is a possible reason. Another reason is that these samples were taken at lower altitudes in valleys compared to higher altitudes in the other two periods. Inspection of Fig. 1 shows the complex terrain surrounding the valleys of Period 3 sampling. Using high-resolution (~ 1 km) terrain data from the U.S. Geological Survey (USGS) Global 30 Arc-Second Elevation (GTOPO30) dataset, we find that the standard deviation of altitude in the $7\text{km} \times 7\text{km}$ region centered at the corresponding observation location correlates well with the observed reactive aromatics with a R^2 value of 0.55 (Fig. 8), which suggests that pollution transport is strongly enhanced by the effects of complex terrain. The horizontal resolution of 36 km used in this study is inadequate to simulate this effect. Model resolution as high as 1 km appears to be necessary to capture the observed feature but the computational resource requirement will be exceptionally large for a global model such as that used for CFSR. [Other issues related to complex terrains in this region were also discussed by previous studies \(Maussion et al., 2011; Ménéguez et al., 2013; He et al., 2014; Kumar et al., 2015\).](#) The effects of complex terrain may have also affected the observations of Periods 1 and 2 but to a smaller extent since the terrain variation is lower and sampling altitude is higher in those periods._

4. Conclusions and implications for climate studies

We apply the REAM model to analyze in situ observations of reactive aromatics across the Tibetan Plateau. Top-down estimate using SCIAMACHY CHOCHO observations suggests that the a priori inventory for aromatics emissions is low by a factor of 2 to 6 over the industrialized Indo-Gangetic Plain. Application of the top-down emission estimate greatly reduces the low bias of the model during Period 2. Model results suggest that the second half of Period 2 is characterized by rapid trans-Himalaya transport from India and nearby regions driven by the presence of a cut-off low system in the upper troposphere.

Model performance for Periods 1 and 3 is poor compared to Period 2 and employing top-down emission estimates does not significantly improve the model simulation of these periods. In situ observations show much stronger surface wind than simulated in the model during Period 1. The lack of radiosonde observations in the interior of the Tibetan Plateau is likely the reason that a cut-off low system, the scale of which is much less than the mid-latitude Rossby wave, is not simulated by the T382 (~38 km) CSFR reanalysis. Consequently, trans-Himalaya transport is greatly underestimated in the model. Sampling of Period 3 is in valleys surrounded by complex terrain. Although observed surface wind is weak, we find that reactive

aromatics concentrations are strongly correlated with the complexity of surrounding terrain, implying enhanced pollution transport by terrain driven mixing. Model simulations at a resolution of 36 km are inadequate for simulating the terrain effect.

The height of the Tibetan Plateau is a natural barrier for pollution transport into this pristine region. This geographical feature is also a challenge for regional and global model simulations. In this study, we use short-lived reactive aromatics as proxies to evaluate model simulated transport to the Tibetan Plateau on the basis of in situ observations. After correcting for the emission underestimation using satellite observations, simulated trans-Himalaya transport of proxy species (using WRF assimilated meteorological fields) still has significant low biases for two reasons, (1) poor representation of a cut-off low system, and (2) inadequate representation of terrain effect due to a coarse model resolution. These two transport-related issues likely exist in global climate models; the coarser resolution of climate models than our simulations or CSFR may further worsen the transport biases. Our ~~analysis~~ results imply that pollution transport to the Tibetan Plateau, such as that of BC, is likely to be greatly underestimated in climate models, which was found previously (e.g., He et al., 2014). Further analysis of reanalysis and climate model simulations is required to quantify potential model biases and the resulting effect of simulated BC deposition to glaciers on the Tibetan Plateau due to the transport issues we identified in this study.

Acknowledgements

The modeling analysis of this work was supported by the Atmospheric Chemistry Program of the U.S. National Science Foundation. The observation sampling and analysis were supported by the National Natural Science Foundation of China (No.41472311, 41273107) and the Special Scientific Research Funds for Environmental Protection Commonwealth Section of China (20603020802L). The contributions of the University of Bremen scientists to this manuscript were funded in part by the University and State of Bremen, DLR (German Aerospace), DFG and ESA. MV acknowledges support from the DFG-Research Center / Cluster of Excellence "The Ocean in the Earth System-MARUM". LMAA gratefully acknowledges the funding support by the German Academic Exchange Service (DAAD).

References

- Alvarado, L. M. A., Richter, A., Vrekoussis, M., Wittrock, F., Hilboll, A., Schreier, S. F., and Burrows, J. P.: An improved glyoxal retrieval from OMI measurements, *Atmos. Meas. Tech.*, 7, 4133-4150, doi: 10.5194/amt-7-4133-2014, 2014.
- Alvarado, L. M. A.: Investigating the role of glyoxal using satellite and MAX-DOAS measurements, Ph.D. thesis, University of Bremen, <http://elib.suub.uni-bremen.de/edocs/00105347-1.pdf>, 2016
- Andreae, M. O., and Merlet, P.: Emission of trace gases and aerosols from biomass burning, *Glob. Biogeochem. Cycles*, 15, 955-966, doi: 10.1029/2000GB001382, 2001.
- Atkinson, R.: Atmospheric chemistry of VOCs and NO_x, *Atmos. Environ.*, 34, 2063-2101, doi: 10.1016/S1352-2310(99)00460-4, 2000.
- Balk, D. L., Deichmann, U., Yetman, G., Pozzi, F., Hay, S. I., and Nelson, A.: Determining Global Population Distribution: Methods, Applications and Data, *Adv. Parasitol.*, 62, 119-156, doi: 10.1016/S0065-308X(05)62004-0, 2006.
- Barnett, T. P., Adam, J. C., and Lettenmaier, D. P.: Potential impacts of a warming climate on water availability in snow-dominated regions, *Nature*, 438, 303-309, doi: 10.1038/nature04141, 2005.
- [Bey, I., Jacob, D. J., Yantosca, R. M., Logan, J. A., Field, B. D., Fiore, A. M., Li, Q. B., Liu, H. G. Y., Mickley, L. J., and Schultz, M. G.: Global modeling of tropospheric chemistry with assimilated meteorology: Model description and evaluation, *J. Geophys. Res.-Atmos.*, 106, 23073-23095, doi: 10.1029/2001jd000807, 2001.](#)
- Bond, T. C., Bhardwaj, E., Dong, R., Jogani, R., Jung, S., Roden, C., Streets, D. G., and Trautmann, N. M.: Historical emissions of black and organic carbon aerosol from energy-related combustion, 1850–2000, *Glob. Biogeochem. Cycles*, 21, GB2018, doi: 10.1029/2006GB002840, 2007.
- Bovensmann, H., Burrows, J. P., Buchwitz, M., Frerick, J., Noël, S., Rozanov, V. V., Chance, K. V., and Goede, A. P. H.: SCIAMACHY: Mission Objectives and Measurement Modes, *J. Atmos. Sci.*, 56, 127-150, 1999.

Burrows, J. P., Hölzle, E., Goede, A. P. H., Visser, H., and Fricke, W.: Earth Observation SCIAMACHY—scanning imaging absorption spectrometer for atmospheric cartography, *Acta Astronautica*, 35, 445-451, doi: 10.1016/0094-5765(94)00278-T, 1995.

Cabrera-Perez, D., Taraborrelli, D., Sander, R., and Pozzer, A.: Global atmospheric budget of simple monocyclic aromatic compounds, *Atmos. Chem. Phys.*, 16, 6931-6947, doi: 10.5194/acp-16-6931-2016, 2016.

Cagliari, J., Fedrizzi, F., Rodrigues Finotti, A., Echevengua Teixeira, C., and do Nascimento Filho, I.: Volatilization of monoaromatic compounds (benzene, toluene, and xylenes; BTX) from gasoline: Effect of the ethanol, *Environ. Toxicol. Chem.*, 29, 808-812, doi: 10.1002/etc.111, 2010.

Choi, Y., Wang, Y., Zeng, T., Martin, R. V., Kurosu, T. P., and Chance, K.: Evidence of lightning NO_x and convective transport of pollutants in satellite observations over North America, *Geophys. Res. Lett.*, 32, L02805, doi: 10.1029/2004GL021436, 2005.

Choi, Y., Wang, Y., Yang, Q., Cunnold, D., Zeng, T., Shim, C., Luo, M., Eldering, A., Bucsela, E., and Gleason, J.: Spring to summer northward migration of high O₃ over the western North Atlantic, *Geophys. Res. Lett.*, 35, L04818, doi: 10.1029/2007GL032276, 2008a.

Choi, Y., Wang, Y., Zeng, T., Cunnold, D., Yang, E. S., Martin, R., Chance, K., Thouret, V., and Edgerton, E.: Springtime transitions of NO₂, CO, and O₃ over North America: Model evaluation and analysis, *J. Geophys. Res.-Atmos.*, 113, 16, doi: 10.1029/2007jd009632, 2008b.

[CIESIN \(Center for International Earth Science Information Network\), C. C. U., International Food Policy Research Institute, I., The World, B., and Centro Internacional de Agricultura Tropical, C.: Global Rural-Urban Mapping Project, Version 1 \(GRUMPv1\): Population Density Grid, NASA Socioeconomic Data and Applications Center \(SEDAC\), Palisades, NY, doi: 10.7927/H4R20Z93, 2011.](#)

[CIESIN \(Center for International Earth Science Information Network\), C. C. U.: Gridded Population of the World, Version 4 \(GPWv4\): Population Density Adjusted to Match 2015 Revision UN WPP Country Totals, NASA Socioeconomic Data and Applications Center \(SEDAC\), Palisades, NY, doi: 10.7927/H4HX19NJ, 2016.](#)

Cong, Z., Kang, S., Gao, S., Zhang, Y., Li, Q., and Kawamura, K.: Historical Trends of Atmospheric Black Carbon on Tibetan Plateau as Reconstructed from a 150-Year Lake Sediment Record, *Environ. Sci. Technol.*, 47, 2579-2586, doi: 10.1021/es3048202, 2013.

Cong, Z., Kawamura, K., Kang, S., and Fu, P.: Penetration of biomass-burning emissions from South Asia through the Himalayas: new insights from atmospheric organic acids, *Sci. Rep.*, 5, doi: 10.1038/srep09580, 2015.

[Dumka, U. C., Moorthy, K. K., Kumar, R., Hegde, P., Sagar, R., Pant, P., Singh, N., and Babu, S. S.: Characteristics of aerosol black carbon mass concentration over a high altitude location in the Central Himalayas from multi-year measurements, *Atmos. Res.*, 96, 510-521, doi: 10.1016/j.atmosres.2009.12.010, 2010.](#)

- Fu, T.-M., Jacob, D. J., Wittrock, F., Burrows, J. P., Vrekoussis, M., and Henze, D. K.: Global budgets of atmospheric glyoxal and methylglyoxal, and implications for formation of secondary organic aerosols, *J. Geophys. Res.*, 113, doi: 10.1029/2007jd009505, 2008.
- Gray, B. A., Wang, Y., Gu, D., Bandy, A., Mauldin, L., Clarke, A., Alexander, B., and Davis, D. D.: Sources, transport, and sinks of SO₂ over the equatorial Pacific during the Pacific Atmospheric Sulfur Experiment, *J. Atmos. Chem.*, 68, 27-53, doi: 10.1007/s10874-010-9177-7, 2011.
- Gu, D. S., Wang, Y. H., Smeltzer, C., and Liu, Z.: Reduction in NO_x Emission Trends over China: Regional and Seasonal Variations, *Environ. Sci. Technol.*, 47, 12912-12919, doi: 10.1021/es401727e, 2013.
- Gu, D., Wang, Y., Smeltzer, C., and Boersma, K. F.: Anthropogenic emissions of NO_x over China: Reconciling the difference of inverse modeling results using GOME-2 and OMI measurements, *J. Geophys. Res.-Atmos.*, 119, 2014JD021644, doi: 10.1002/2014JD021644, 2014.
- [Gu, D., Wang, Y., Yin, R., Zhang, Y., and Smeltzer, C.: Inverse modelling of NO_x emissions over eastern China: uncertainties due to chemical non-linearity, *Atmos. Meas. Tech.*, 9, 5193-5201, doi: 10.5194/amt-9-5193-2016, 2016.](#)
- Guenther, A. B., Jiang, X., Heald, C. L., Sakulyanontvittaya, T., Duhl, T., Emmons, L. K., and Wang, X.: The Model of Emissions of Gases and Aerosols from Nature version 2.1 (MEGAN2.1): an extended and updated framework for modeling biogenic emissions, *Geosci. Model Dev.*, 5, 1471-1492, doi: 10.5194/gmd-5-1471-2012, 2012.
- Hansen, J., and Nazarenko, L.: Soot climate forcing via snow and ice albedos, *Proc. Natl. Acad. Sci. USA*, 101, 423-428, doi: 10.1073/pnas.2237157100, 2004.
- He, C., Li, Q. B., Liou, K. N., Zhang, J., Qi, L., Mao, Y., Gao, M., Lu, Z., Streets, D. G., Zhang, Q., Sarin, M. M., and Ram, K.: A global 3-D CTM evaluation of black carbon in the Tibetan Plateau, *Atmos. Chem. Phys.*, 14, 7091-7112, doi: 10.5194/acp-14-7091-2014, 2014.
- Henze, D. K., Seinfeld, J. H., Ng, N. L., Kroll, J. H., Fu, T. M., Jacob, D. J., and Heald, C. L.: Global modeling of secondary organic aerosol formation from aromatic hydrocarbons: high- vs. low-yield pathways, *Atmos. Chem. Phys.*, 8, 2405-2420, doi: 10.5194/acp-8-2405-2008, 2008.
- Hindman, E. E., and Upadhyay, B. P.: Air pollution transport in the Himalayas of Nepal and Tibet during the 1995–1996 dry season, *Atmos. Environ.*, 36, 727-739, doi: 10.1016/S1352-2310(01)00495-2, 2002.
- Hoskins, B. J., McIntyre, M. E., and Robertson, A. W.: On the use and significance of isentropic potential vorticity maps, *Q. J. R. Meteorol. Soc.*, 111, 877-946, doi: 10.1002/qj.49711147002, 1985.
- [Ji, Z., Kang, S., Cong, Z., Zhang, Q., and Yao, T.: Simulation of carbonaceous aerosols over the Third Pole and adjacent regions: distribution, transportation, deposition, and climatic effects, *Clim. Dyn.*, 45, 2831-2846, doi: 10.1007/s00382-015-2509-1, 2015.](#)
- [Kang, S., Huang, J., Wang, F., Zhang, Q., Zhang, Y., Li, C., Wang, L., Chen, P., Sharma, C. M., Li, Q., Sillanpää, M., Hou, J., Xu, B., and Guo, J.: Atmospheric Mercury Depositional Chronology Reconstructed from Lake Sediments and Ice Core in the Himalayas and Tibetan Plateau, *Environ. Sci. Technol.*, 50, 2859-2869, doi: 10.1021/acs.est.5b04172, 2016.](#)

- Kehrwald, N. M., Thompson, L. G., Tandong, Y., Mosley-Thompson, E., Schotterer, U., Alfimov, V., Beer, J., Eikenberg, J., and Davis, M. E.: Mass loss on Himalayan glacier endangers water resources, *Geophys. Res. Lett.*, 35, L22503, doi: 10.1029/2008GL035556, 2008.
- Kopacz, M., Mauzerall, D. L., Wang, J., Leibensperger, E. M., Henze, D. K., and Singh, K.: Origin and radiative forcing of black carbon transported to the Himalayas and Tibetan Plateau, *Atmos. Chem. Phys.*, 11, 2837-2852, doi: 10.5194/acp-11-2837-2011, 2011.
- [Kumar, R., Barth, M. C., Pfister, G. G., Nair, V. S., Ghude, S. D., and Ojha, N.: What controls the seasonal cycle of black carbon aerosols in India?, *J. Geophys. Res.: Atmospheres*, 120, 7788-7812, doi: 10.1002/2015JD023298, 2015.](#)
- [Lawrence, M. G., and Lelieveld, J.: Atmospheric pollutant outflow from southern Asia: a review, *Atmos. Chem. Phys.*, 10, 11017-11096, doi: 10.5194/acp-10-11017-2010, 2010.](#)
- Lerot, C., Stavrou, T., De Smedt, I., Muller, J. F., and Van Roozendaal, M.: Glyoxal vertical columns from GOME-2 backscattered light measurements and comparisons with a global model, *Atmos. Chem. Phys.*, 10, 12059-12072, doi: 10.5194/acp-10-12059-2010, 2010.
- [Li, C., Bosch, C., Kang, S., Andersson, A., Chen, P., Zhang, Q., Cong, Z., Chen, B., Qin, D., and Gustafsson, Ö.: Sources of black carbon to the Himalayan–Tibetan Plateau glaciers, *Nat. Commun.*, 7, 12574, doi: 10.1038/ncomms12574, 2016.](#)
- Li, M., Zhang, Q., Streets, D. G., He, K. B., Cheng, Y. F., Emmons, L. K., Huo, H., Kang, S. C., Lu, Z., Shao, M., Su, H., Yu, X., and Zhang, Y.: Mapping Asian anthropogenic emissions of non-methane volatile organic compounds to multiple chemical mechanisms, *Atmos. Chem. Phys.*, 14, 5617-5638, doi: 10.5194/acp-14-5617-2014, 2014.
- [Li, M., Zhang, Q., Kurokawa, J., Woo, J. H., He, K. B., Lu, Z., Ohara, T., Song, Y., Streets, D. G., Carmichael, G. R., Cheng, Y. F., Hong, C. P., Huo, H., Jiang, X. J., Kang, S. C., Liu, F., Su, H., and Zheng, B.: MIX: a mosaic Asian anthropogenic emission inventory for the MICS-Asia and the HTAP projects, *Atmos. Chem. Phys. Discuss.*, 2015, 34813-34869, doi: 10.5194/acpd-15-34813-2015, 2015.](#)
- Liu, Z., Wang, Y., Gu, D., Zhao, C., Huey, L. G., Stickel, R., Liao, J., Shao, M., Zhu, T., Zeng, L., Liu, S.-C., Chang, C.-C., Amoroso, A., and Costabile, F.: Evidence of Reactive Aromatics As a Major Source of Peroxy Acetyl Nitrate over China, *Environ. Sci. Technol.*, 44, 7017-7022, doi: 10.1021/es1007966, 2010.
- Liu, Z., Wang, Y., Gu, D., Zhao, C., Huey, L. G., Stickel, R., Liao, J., Shao, M., Zhu, T., Zeng, L., Amoroso, A., Costabile, F., Chang, C. C., and Liu, S. C.: Summertime photochemistry during CAREBeijing-2007: ROx budgets and O₃ formation, *Atmos. Chem. Phys.*, 12, 7737-7752, doi: 10.5194/acp-12-7737-2012, 2012a.
- Liu, Z., Wang, Y., Vrekoussis, M., Richter, A., Wittrock, F., Burrows, J. P., Shao, M., Chang, C.-C., Liu, S.-C., Wang, H., and Chen, C.: Exploring the missing source of glyoxal (CHOCHO) over China, *Geophys. Res. Lett.*, 39, L10812, doi: 10.1029/2012GL051645, 2012b.

- Liu, Z., Wang, Y., Costabile, F., Amoroso, A., Zhao, C., Huey, L. G., Stickel, R., Liao, J., and Zhu, T.: Evidence of Aerosols as a Media for Rapid Daytime HONO Production over China, *Environ. Sci. Technol.*, 48, 14386-14391, doi: 10.1021/es504163z, 2014.
- Lu, Z., Streets, D. G., Zhang, Q., and Wang, S.: A novel back-trajectory analysis of the origin of black carbon transported to the Himalayas and Tibetan Plateau during 1996–2010, *Geophys. Res. Lett.*, 39, L01809, doi: 10.1029/2011GL049903, 2012.
- Lutz, A. F., Immerzeel, W. W., Shrestha, A. B., and Bierkens, M. F. P.: Consistent increase in High Asia's runoff due to increasing glacier melt and precipitation, *Nat. Clim. Chang.*, 4, 587-592, doi: 10.1038/nclimate2237, 2014.
- [Lüthi, Z. L., Škerlak, B., Kim, S. W., Lauer, A., Mues, A., Rupakheti, M., and Kang, S.: Atmospheric brown clouds reach the Tibetan Plateau by crossing the Himalayas, *Atmos. Chem. Phys.*, 15, 6007-6021, doi: 10.5194/acp-15-6007-2015, 2015.](#)
- [Maussion, F., Scherer, D., Finkelnburg, R., Richters, J., Yang, W., and Yao, T.: WRF simulation of a precipitation event over the Tibetan Plateau, China – an assessment using remote sensing and ground observations, *Hydrol. Earth Syst. Sci.*, 15, 1795-1817, doi: 10.5194/hess-15-1795-2011, 2011.](#)
- [Ménégoz, M., Gallée, H., and Jacobi, H. W.: Precipitation and snow cover in the Himalaya: from reanalysis to regional climate simulations, *Hydrol. Earth Syst. Sci.*, 17, 3921-3936, doi: 10.5194/hess-17-3921-2013, 2013.](#)
- [Menon, S., Hansen, J., Nazarenko, L., and Luo, Y.: Climate Effects of Black Carbon Aerosols in China and India, *Science*, 297, 2250-2253, doi: 10.1126/science.1075159, 2002.](#)
- Ming, J., Xiao, C., Cachier, H., Qin, D., Qin, X., Li, Z., and Pu, J.: Black Carbon (BC) in the snow of glaciers in west China and its potential effects on albedos, *Atmos. Res.*, 92, 114-123, doi: 10.1016/j.atmosres.2008.09.007, 2009.
- Myriokefalitakis, S., Vrekoussis, M., Tsigaridis, K., Wittrock, F., Richter, A., Brühl, C., Volkamer, R., Burrows, J. P., and Kanakidou, M.: The influence of natural and anthropogenic secondary sources on the glyoxal global distribution, *Atmos. Chem. Phys.*, 8, 4965-4981, doi: 10.5194/acp-8-4965-2008, 2008.
- [N. S. S. O. \(NSSO\), Household Consumption of various Goods and Services in India, \(July 2009-June 2010\), vol. KI of 69th round. National Sample Survey Office, Ministry of Statistics & Programme Implementation, Government of India, 2012a](#)
- [N. S. S. O. \(NSSO\), Energy Sources of Indian Households, \(July 2009-June 2010\), vol. KI of 69th round. National Sample Survey Office, Ministry of Statistics & Programme Implementation, Government of India, 2012b](#)
- Ohara, T., Akimoto, H., Kurokawa, J.-I., Horii, N., Yamaji, K., Yan, X., and Hayasaka, T.: An Asian emission inventory of anthropogenic emission sources for the period 1980–2020, *Atmos. Chem. Phys.*, 7, 4419-4444, doi: 10.5194/acp-7-4419-2007, 2007.

[Pettersson, E., Boman, C., Westerholm, R., Boström, D., and Nordin, A.: Stove Performance and Emission Characteristics in Residential Wood Log and Pellet Combustion, Part 2: Wood Stove, Energy Fuels, 25, 315-323, doi: 10.1021/ef1007787, 2011.](#)

Ramanathan, V., and Carmichael, G.: Global and regional climate changes due to black carbon, *Nat. Geosci.*, 1, 221-227, doi: 10.1038/ngeo156, 2008.

Sack, T. M., Steele, D. H., Hammerstrom, K., and Remmers, J.: A survey of household products for volatile organic compounds, *Atmos. Environ. Part A*, 26, 1063-1070, doi: 10.1016/0960-1686(92)90038-M, 1992.

Saha, S., Moorthi, S., Pan, H.-L., Wu, X., Wang, J., Nadiga, S., Tripp, P., Kistler, R., Woollen, J., Behringer, D., Liu, H., Stokes, D., Grumbine, R., Gayno, G., Wang, J., Hou, Y.-T., Chuang, H.-Y., Juang, H.-M. H., Sela, J., Iredell, M., Treadon, R., Kleist, D., Van Delst, P., Keyser, D., Derber, J., Ek, M., Meng, J., Wei, H., Yang, R., Lord, S., Van Den Dool, H., Kumar, A., Wang, W., Long, C., Chelliah, M., Xue, Y., Huang, B., Schemm, J.-K., Ebisuzaki, W., Lin, R., Xie, P., Chen, M., Zhou, S., Higgins, W., Zou, C.-Z., Liu, Q., Chen, Y., Han, Y., Cucurull, L., Reynolds, R. W., Rutledge, G., and Goldberg, M.: The NCEP Climate Forecast System Reanalysis, *Bull. Am. Meteorol. Soc.*, 91, 1015-1057, doi: 10.1175/2010BAMS3001.1, 2010.

Singh, P., and Bengtsson, L.: Hydrological sensitivity of a large Himalayan basin to climate change, *Hydrol. Process.*, 18, 2363-2385, doi: 10.1002/hyp.1468, 2004.

Stavrakou, T., Muller, J. F., De Smedt, I., Van Roozendaal, M., Kanakidou, M., Vrekoussis, M., Wittrock, F., Richter, A., and Burrows, J. P.: The continental source of glyoxal estimated by the synergistic use of spaceborne measurements and inverse modelling, *Atmos. Chem. Phys.*, 9, 8431-8446, doi: 10.5194/acp-9-8431-2009, 2009.

van der Werf, G. R., Randerson, J. T., Giglio, L., Collatz, G. J., Mu, M., Kasibhatla, P. S., Morton, D. C., DeFries, R. S., Jin, Y., and van Leeuwen, T. T.: Global fire emissions and the contribution of deforestation, savanna, forest, agricultural, and peat fires (1997–2009), *Atmos. Chem. Phys.*, 10, 11707-11735, doi: 10.5194/acp-10-11707-2010, 2010.

Volkamer, R., Molina, L. T., Molina, M. J., Shirley, T., and Brune, W. H.: DOAS measurement of glyoxal as an indicator for fast VOC chemistry in urban air, *Geophys. Res. Lett.*, 32, L08806, doi: 10.1029/2005GL022616, 2005.

Vrekoussis, M., Wittrock, F., Richter, A., and Burrows, J. P.: Temporal and spatial variability of glyoxal as observed from space, *Atmos. Chem. Phys.*, 9, 4485-4504, doi: 10.5194/acp-9-4485-2009, 2009.

[Wang, M., Xu, B., Wang, N., Cao, J., Tie, X., Wang, H., Zhu, C., and Yang, W.: Two distinct patterns of seasonal variation of airborne black carbon over Tibetan Plateau, *Sci. Total Environ.*, 573, 1041-1052, doi: 10.1016/j.scitotenv.2016.08.184, 2016.](#)

Wang, X., Gong, P., Sheng, J., Joswiak, D. R., and Yao, T.: Long-range atmospheric transport of particulate Polycyclic Aromatic Hydrocarbons and the incursion of aerosols to the southeast Tibetan Plateau, *Atmos. Environ.*, 115, 124-131, doi: 10.1016/j.atmosenv.2015.04.050, 2015.

- Wang, Y., Choi, Y., Zeng, T., Ridley, B., Blake, N., Blake, D., and Flocke, F.: Late-spring increase of trans-Pacific pollution transport in the upper troposphere, *Geophys. Res. Lett.*, 33, L01811, doi: 10.1029/2005GL024975, 2006.
- Wang, Y., Choi, Y., Zeng, T., Davis, D., Buhr, M., Gregory Huey, L., and Neff, W.: Assessing the photochemical impact of snow emissions over Antarctica during ANTCI 2003, *Atmos. Environ.*, 41, 3944-3958, doi: 10.1016/j.atmosenv.2007.01.056, 2007.
- Wittrock, F., Richter, A., Oetjen, H., Burrows, J. P., Kanakidou, M., Myriokefalitakis, S., Volkamer, R., Beirle, S., Platt, U., and Wagner, T.: Simultaneous global observations of glyoxal and formaldehyde from space, *Geophys. Res. Lett.*, 33, 5, doi: 10.1029/2006gl026310, 2006.
- Xu, B., Cao, J., Hansen, J., Yao, T., Joswia, D. R., Wang, N., Wu, G., Wang, M., Zhao, H., Yang, W., Liu, X., and He, J.: Black soot and the survival of Tibetan glaciers, *Proc. Natl. Acad. Sci. USA*, 106, 22114-22118, doi: 10.1073/pnas.0910444106, 2009.
- Yang, Q., Wang, Y., Zhao, C., Liu, Z., Gustafson, W. I., and Shao, M.: NO_x Emission Reduction and its Effects on Ozone during the 2008 Olympic Games, *Environ. Sci. Technol.*, 45, 6404-6410, doi: 10.1021/es200675v, 2011.
- Yao, T., Wang, Y., Liu, S., Pu, J., Shen, Y., and Lu, A.: Recent glacial retreat in High Asia in China and its impact on water resource in Northwest China, *Sci. China Ser. D*, 47, 1065-1075, doi: 10.1360/03yd0256, 2004.
- [Yasunari, T. J., Bonasoni, P., Laj, P., Fujita, K., Vuillermoz, E., Marinoni, A., Cristofanelli, P., Duchi, R., Tartari, G., and Lau, K. M.: Estimated impact of black carbon deposition during pre-monsoon season from Nepal Climate Observatory – Pyramid data and snow albedo changes over Himalayan glaciers, *Atmos. Chem. Phys.*, 10, 6603-6615, doi: 10.5194/acp-10-6603-2010, 2010.](#)
- Zeng, T., Wang, Y., Chance, K., Browell, E. V., Ridley, B. A., and Atlas, E. L.: Widespread persistent near-surface ozone depletion at northern high latitudes in spring, *Geophys. Res. Lett.*, 30, 2298, doi: 10.1029/2003GL018587, 2003.
- Zeng, T., Wang, Y., Chance, K., Blake, N., Blake, D., and Ridley, B.: Halogen-driven low-altitude O₃ and hydrocarbon losses in spring at northern high latitudes, *J. Geophys. Res.-Atmos.*, 111, D17313, doi: 10.1029/2005JD006706, 2006.
- Zhang, Q., Streets, D. G., Carmichael, G. R., He, K. B., Huo, H., Kannari, A., Klimont, Z., Park, I. S., Reddy, S., Fu, J. S., Chen, D., Duan, L., Lei, Y., Wang, L. T., and Yao, Z. L.: Asian emissions in 2006 for the NASA INTEX-B mission, *Atmos. Chem. Phys.*, 9, 5131-5153, doi: 10.5194/acp-9-5131-2009, 2009.
- Zhang, R., Wang, H., Qian, Y., Rasch, P. J., Easter, R. C., Ma, P. L., Singh, B., Huang, J., and Fu, Q.: Quantifying sources, transport, deposition, and radiative forcing of black carbon over the Himalayas and Tibetan Plateau, *Atmos. Chem. Phys.*, 15, 6205-6223, doi: 10.5194/acp-15-6205-2015, 2015.
- Zhang, Y., Wang, X., Blake, D. R., Li, L., Zhang, Z., Wang, S., Guo, H., Lee, F. S., Gao, B., and Chan, L.: Aromatic hydrocarbons as ozone precursors before and after outbreak of the 2008 financial crisis in the

Pearl River Delta region, south China, *J. Geophys. Res.-Atmos.*, 117, D15306, doi: 10.1029/2011JD017356, 2012.

Zhang, Y., Wang, Y., Gray, B. A., Gu, D., Mauldin, L., Cantrell, C., and Bandy, A.: Surface and free tropospheric sources of methanesulfonic acid over the tropical Pacific Ocean, *Geophys. Res. Lett.*, 41, 2014GL060934, doi: 10.1002/2014GL060934, 2014.

Zhang, Y., and Wang, Y.: Climate-driven ground-level ozone extreme in the fall over the Southeast United States, *Proc. Natl. Acad. Sci. USA*, 113, 10025-10030, doi: 10.1073/pnas.1602563113, 2016.

Zhang, Y., Wang, Y., Chen, G., Smeltzer, C., Crawford, J., Olson, J., Szykman, J., Weinheimer, A. J., Knapp, D. J., Montzka, D. D., Wisthaler, A., Mikoviny, T., Fried, A., and Diskin, G.: Large vertical gradient of reactive nitrogen oxides in the boundary layer: Modeling analysis of DISCOVER-AQ 2011 observations, *J. Geophys. Res.-Atmos.*, 121, 1922-1934, doi: 10.1002/2015JD024203, 2016.

Zhao, C., and Wang, Y.: Assimilated inversion of NO_x emissions over east Asia using OMI NO₂ column measurements, *Geophys. Res. Lett.*, 36, L06805, doi: 10.1029/2008GL037123, 2009.

Zhao, C., Wang, Y., Choi, Y., and Zeng, T.: Summertime impact of convective transport and lightning NO_x production over North America: modeling dependence on meteorological simulations, *Atmos. Chem. Phys.*, 9, 4315-4327, doi: 10.5194/acp-9-4315-2009, 2009a.

Zhao, C., Wang, Y., and Zeng, T.: East China Plains: A “Basin” of Ozone Pollution, *Environ. Sci. Technol.*, 43, 1911-1915, doi: 10.1021/es8027764, 2009b.

Zhao, C., Wang, Y., Yang, Q., Fu, R., Cunnold, D., and Choi, Y.: Impact of East Asian summer monsoon on the air quality over China: View from space, *J. Geophys. Res.-Atmos.*, 115, D09301, doi: 10.1029/2009JD012745, 2010.

[Zhao, Z., Cao, J., Shen, Z., Xu, B., Zhu, C., Chen, L. W. A., Su, X., Liu, S., Han, Y., Wang, G., and Ho, K.: Aerosol particles at a high-altitude site on the Southeast Tibetan Plateau, China: Implications for pollution transport from South Asia, *J. Geophys. Res.-Atmos.*, 118, 11,360-311,375, doi: 10.1002/jgrd.50599, 2013.](#)

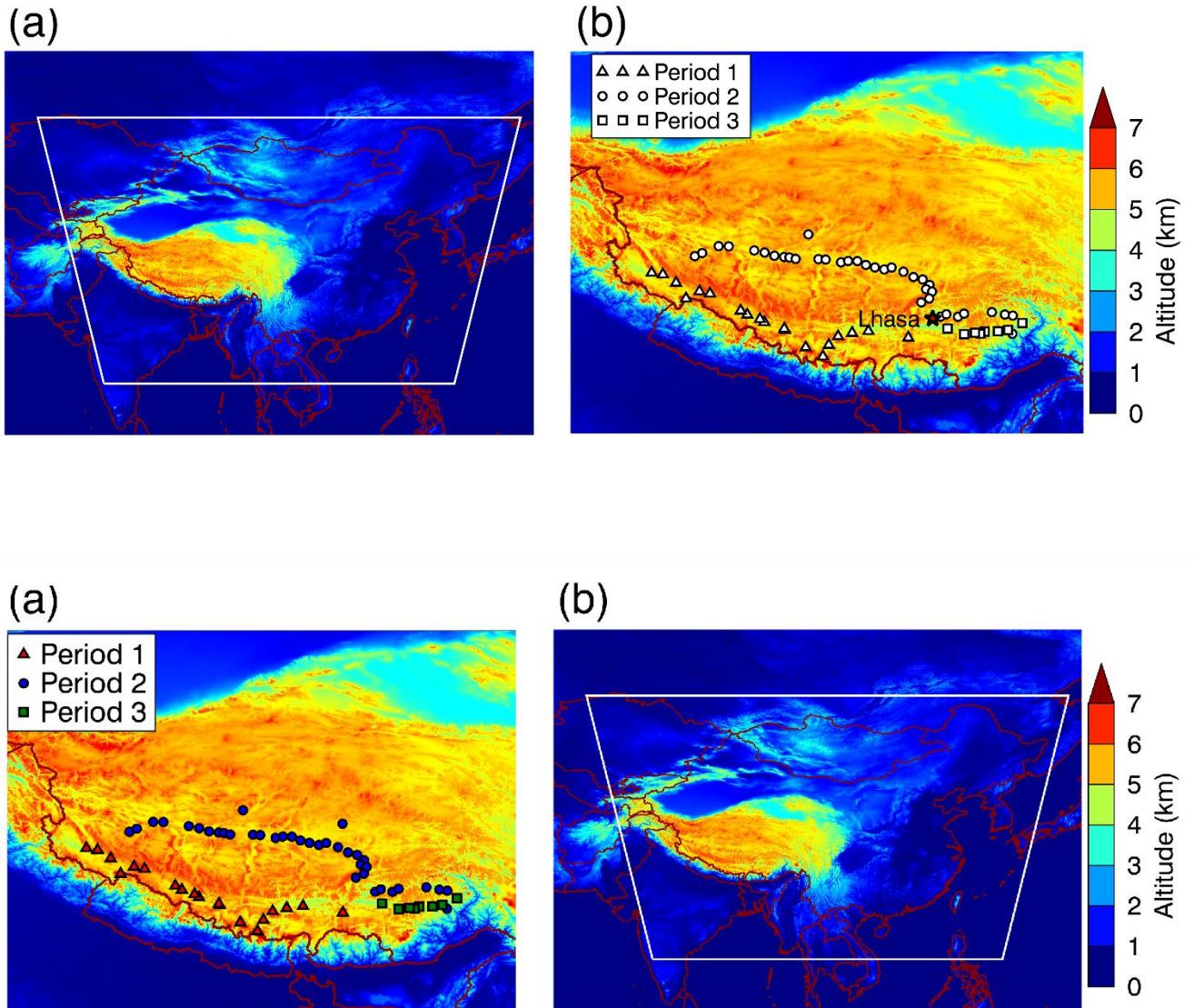


Figure 1: Overview of regions involved in this study. **White polygon in (a) represents the domain margin of the model.** Locations of observations for Period 1 (Oct 13-17, 2010, triangle), Period 2 (Oct 19-24, 2010, circle) and Period 3 (Oct 25, 2010, square) are shown in (a). **White polygon in (b) represents the model domain margin of REAM.** Altitude data from Global Topographic Data (GTOPO30, courtesy of the U.S. Geological Survey) is shown as colored background.

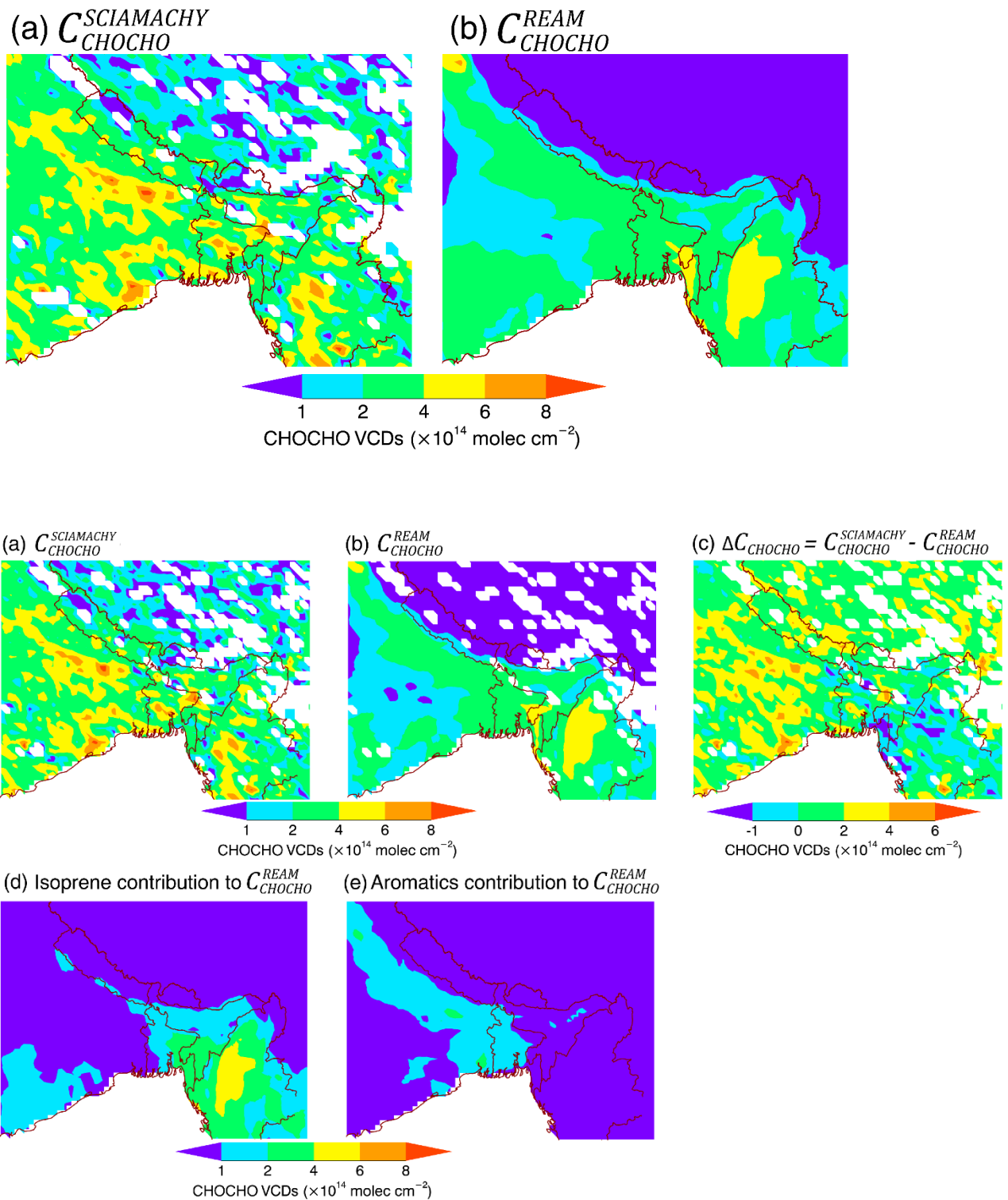


Figure 2: SCIAMACHY observed CHOCHO VCDs (a) and, REAM simulated (b) CHOCHO VCDs, the low bias of simulated CHOCHO VCDs (c), simulated isoprene (d) and aromatics (e) contributions to CHOCHO VCDs using the a priori emissions for October 2010. White areas in the observations denote missing satellite data or ocean. For each valid SCIAMACHY data point, a corresponding model value is sampled in (b) and (c).

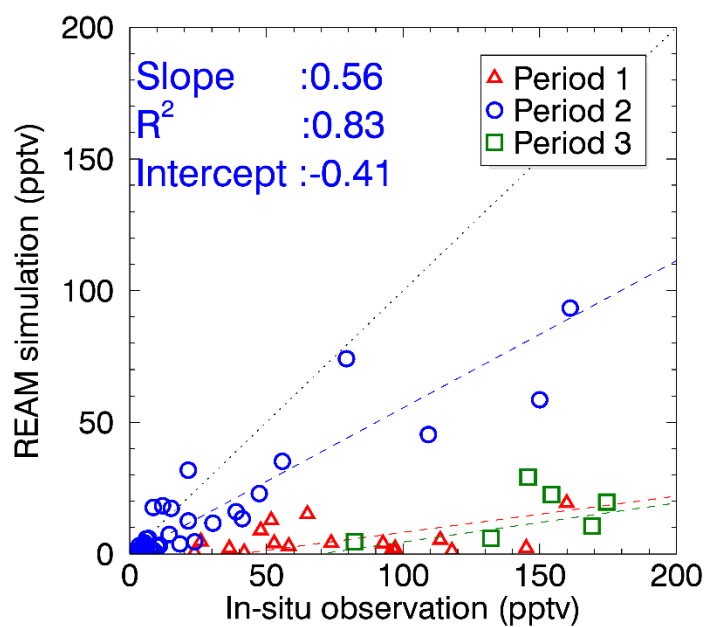
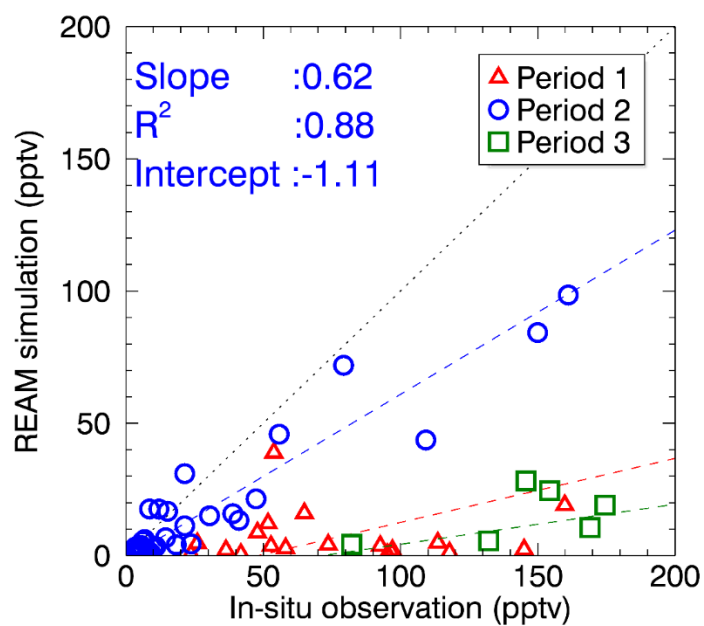
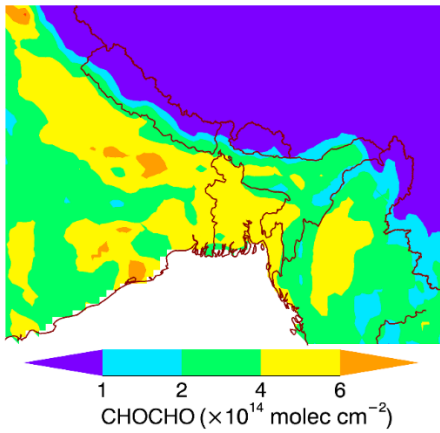
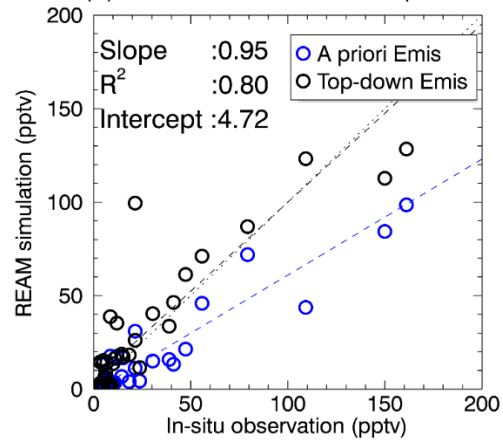


Figure 3: Comparison between REAM simulated reactive aromatics concentrations (Y-axis) and in situ observations (X-axis). REAM results are archived corresponding to the time and location of the observations. Linear regression results for three periods are shown in red (slope=0.2414, $R^2=0.0004$), blue (slope=0.6256, $R^2=0.8883$), and green (slope=0.15, $R^2=0.02$) dashed lines, respectively.

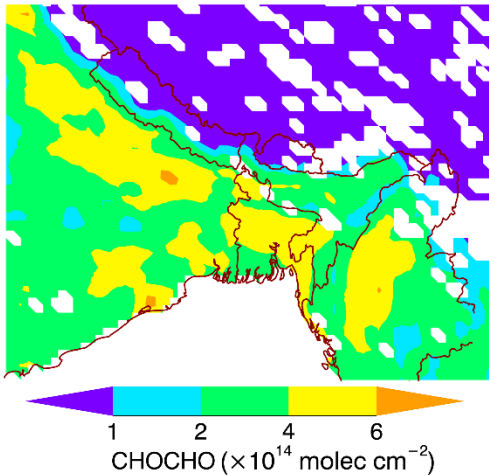
(a) C_{CHOCHO}^{REAM} with top-down emission



(b) Reactive aromatics comparison



(a) C_{CHOCHO}^{REAM} with top-down emission



(b) Reactive aromatics comparison

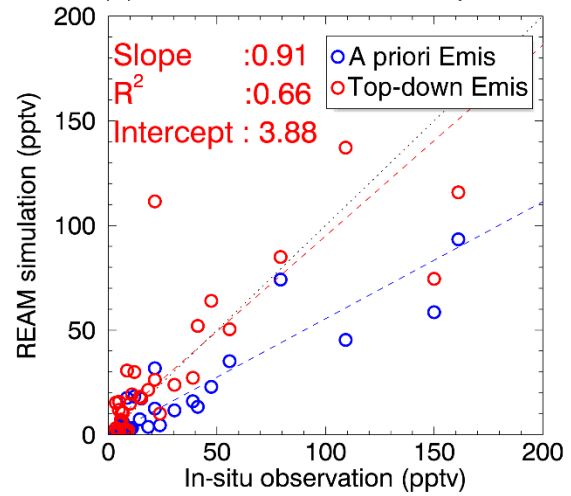


Figure 4: REAM simulated CHOCHO VCDs with top-down emissions (a) and comparison of simulated and observed reactive aromatics concentrations during Period 2 (b). Blue and black circles in panel (b) represent REAM simulation with a priori (slope=0.6256, R^2 =0.8883) and with top-down (slope=0.9591, R^2 =0.8066) emissions, respectively.

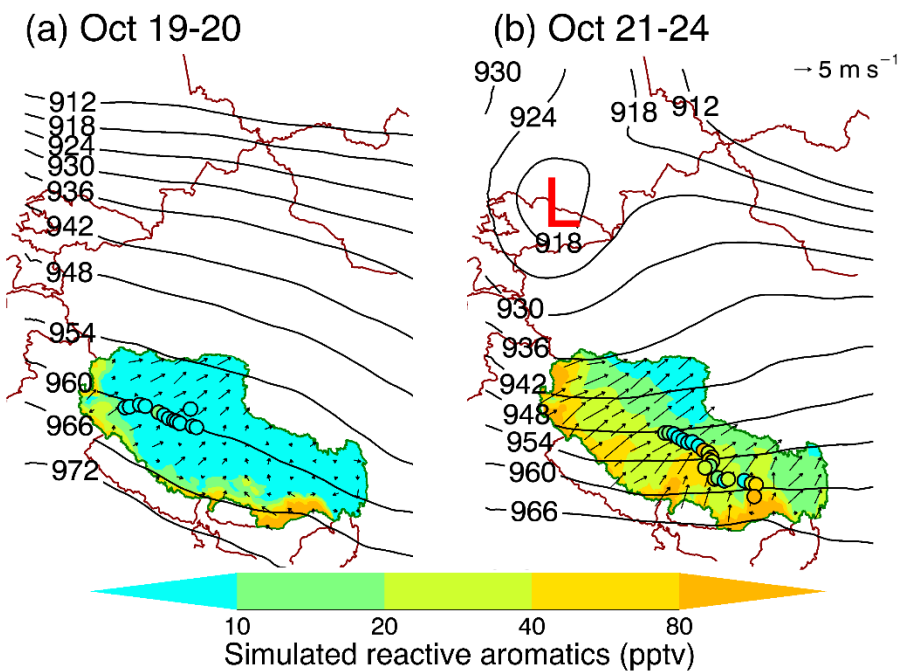
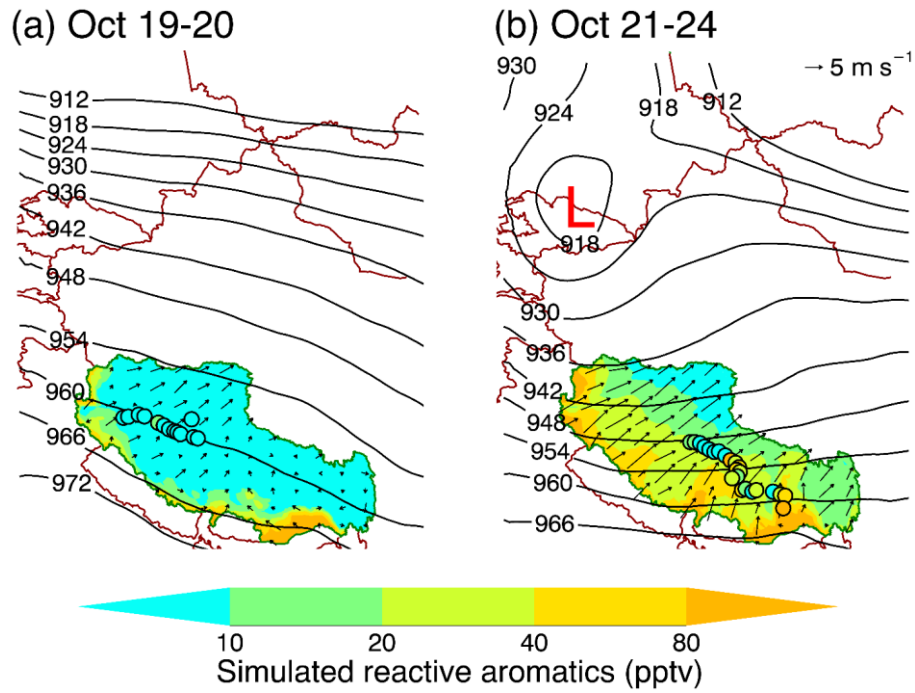
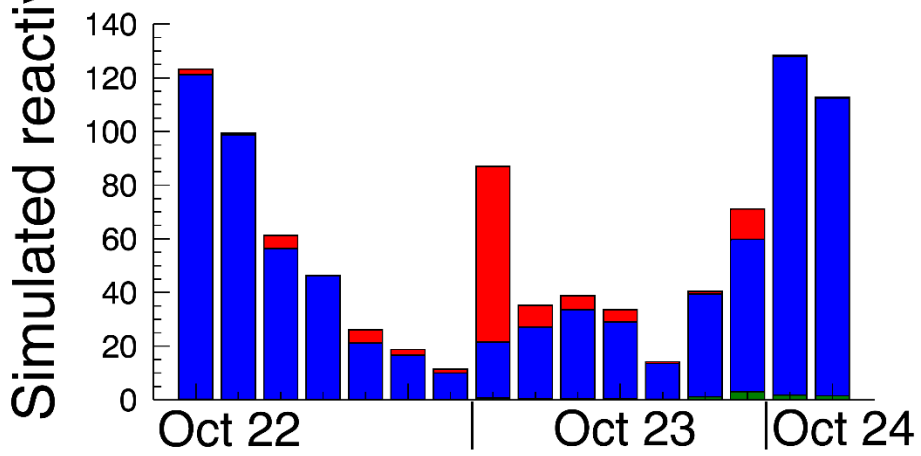
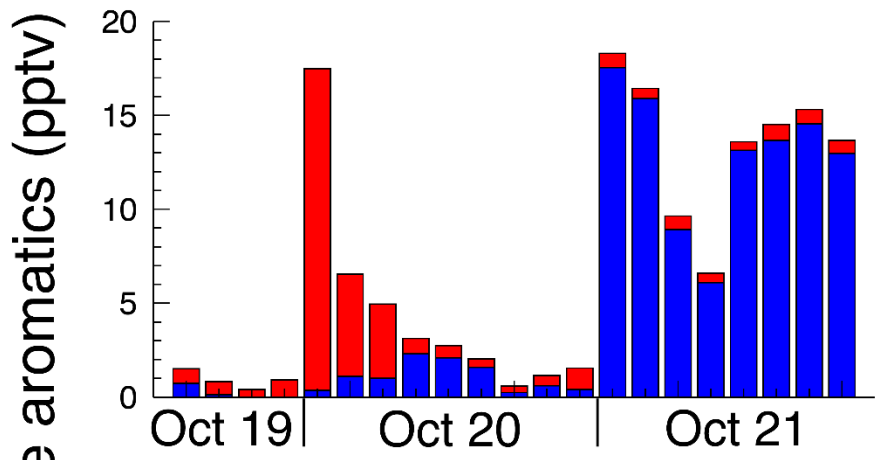


Figure 5: Distributions of WRF simulated surface wind and REAM simulated concentrations of reactive aromatics over the Tibetan Plateau during October 19-20, 2010 (a) and October 21-24, 2010 (b). Circles show the observed reactive aromatics concentrations. Composite distributions of simulated reactive aromatics concentrations and surface wind over Tibet, corresponding to sampling time of the observations, are shown in color and by arrows, respectively. Corresponding WRF simulated 300 hPa geopotential height fields are shown by contour lines. The border of Tibet Autonomous Region is colored green.



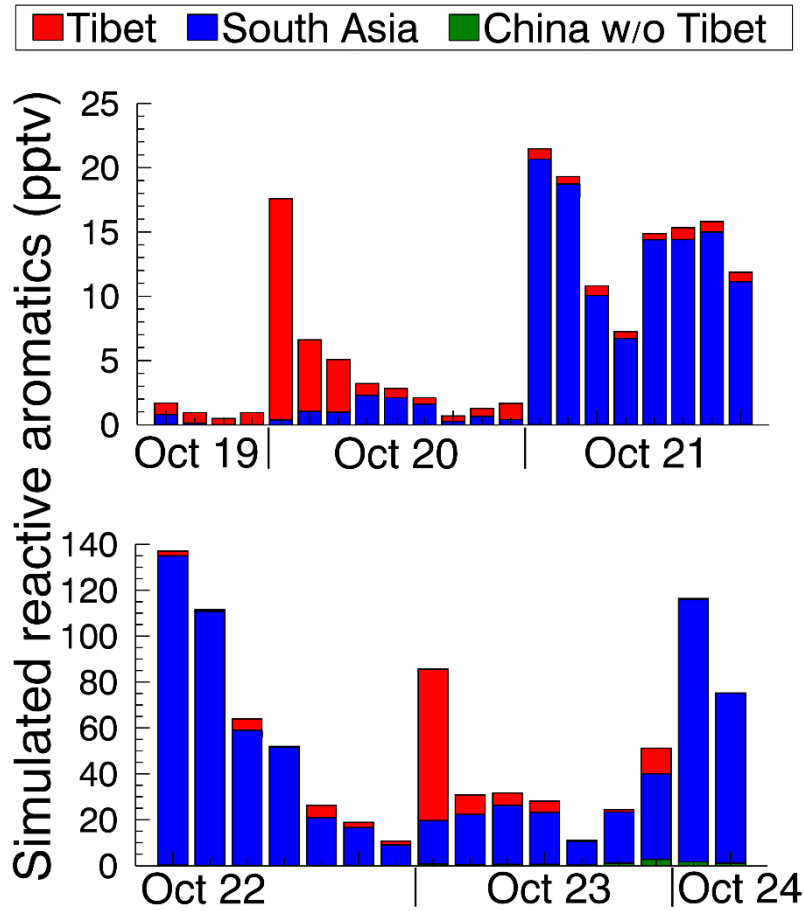
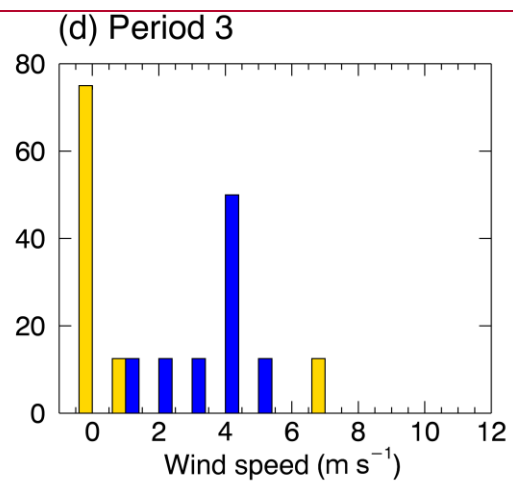
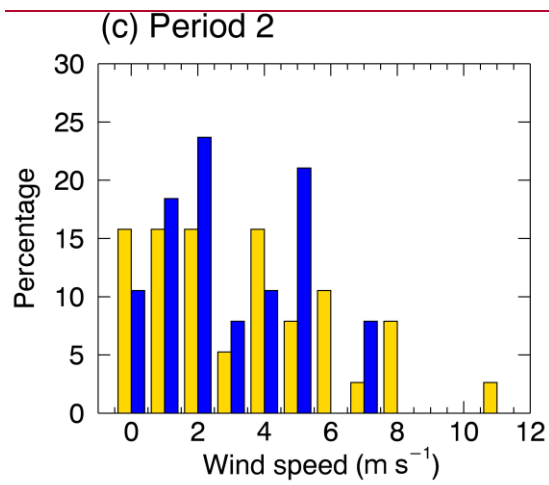
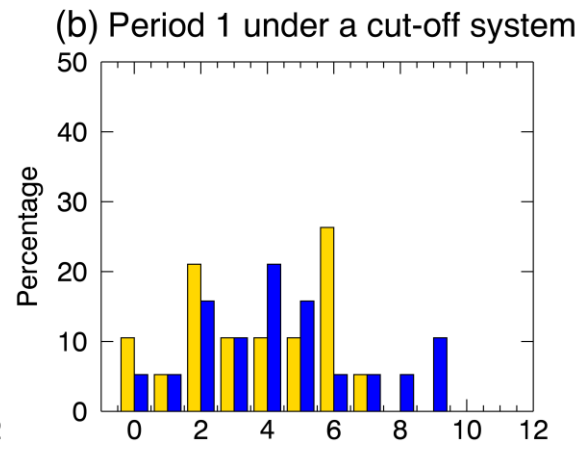
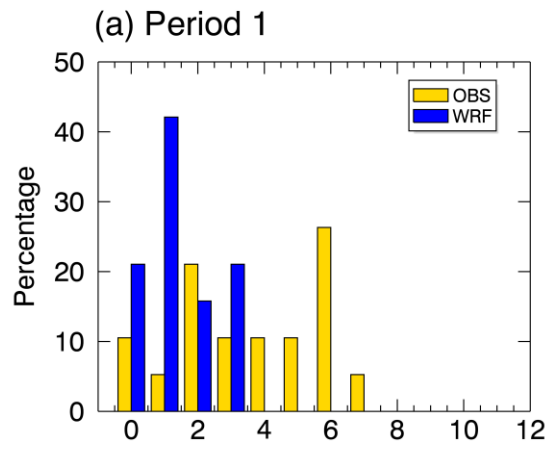


Figure 6: Reactive aromatics emitted from Tibet (red), India and nearby regions (“South Asia”, blue) and China excluding Tibet (“China w/o Tibet”, green) corresponding to the in situ observations in the REAM simulation with top-down emissions. Contributions from the other regions are negligible.



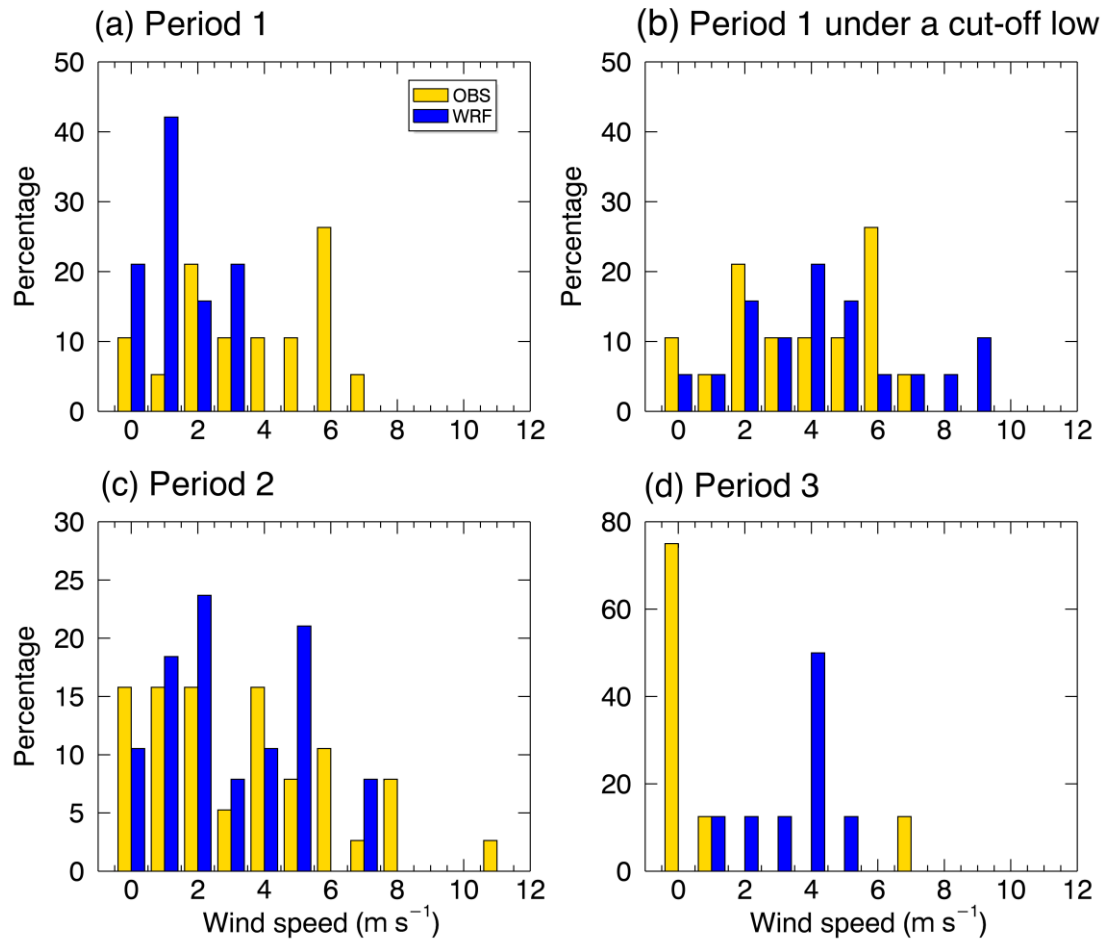


Figure 7: Histograms of observed and simulated surface wind speed for Period 1 (a), Period 2 (c) and Period 3 (d). Panel (b) shows the wind histogram of October 23 with an upper tropospheric ~~cut~~-cut-off low system. Model results are sampled at the same time and location as the observations. In Panel (d), the date information is not used. Wind speed is binned at 1 m/s interval.

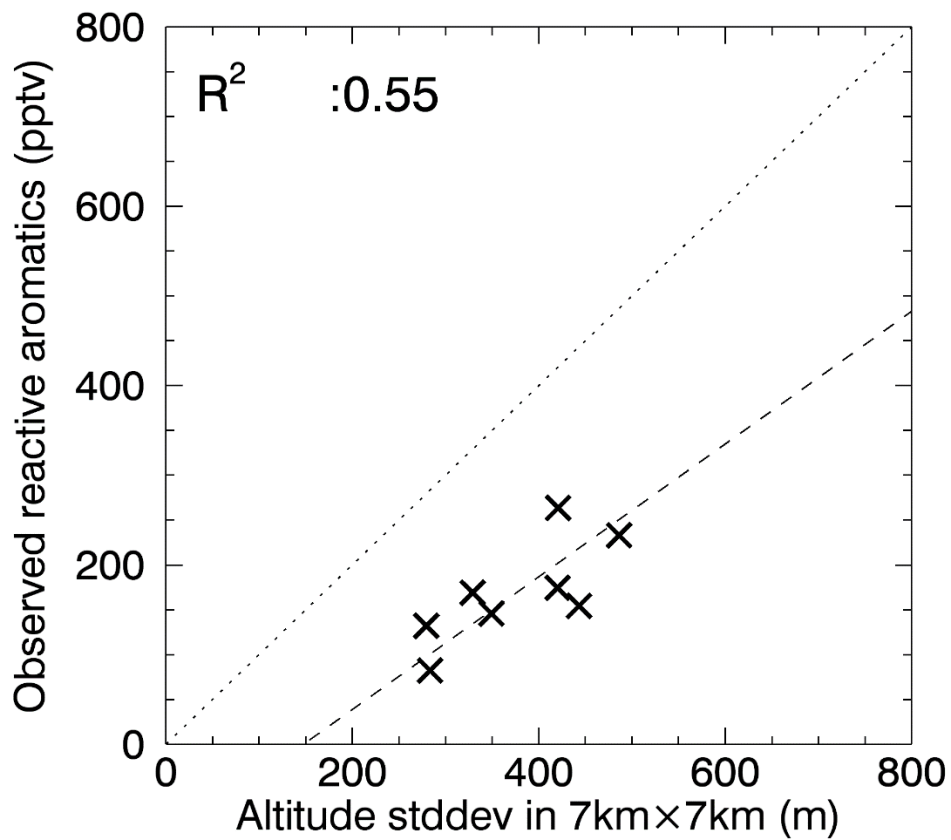


Figure 8: Observed reactive aromatics as a function of terrain complex during Period 3. The latter is computed as the standard deviation of altitude in a 7km x 7km region centered at the sampling location. The dash line denotes a least-squares regression.